

Control of Glucose Utilization in Working Perfused Rat Heart*

(Received for publication, April 22, 1994, and in revised form, July 14, 1994)

Yoshishiro Kashiwaya, Kiyotaka Sato[‡], Naotaka Tsuchiya, Simon Thomas[§], David A. Fell[§], Richard L. Veech[¶], and Janet V. Passonneau

From the National Institute on Alcoholism and Alcohol Abuse, Rockville, Maryland 20895 and the [§]School of Biological and Molecular Sciences, Oxford Brookes University, Headington, Oxford OX3 0BP, United Kingdom

Metabolic control analyses of glucose utilization were performed for four groups of working rat hearts perfused with Krebs-Henseleit buffer containing 10 mM glucose only, or with the addition of 4 mM D-β-hydroxybutyrate/1 mM acetoacetate, 100 nM insulin (0.05 unit/ml), or both. Net glycogen breakdown occurred in the glucose group only and was converted to net glycogen synthesis in the presence of all additions. The flux of [2-³H]glucose through P-glucosomerase (EC 5.3.1.9) was reduced with ketones, elevated with insulin, and unchanged with the combination. Net glycolytic flux was reduced in the presence of ketones and the combination.

The flux control coefficients were determined for the portion of the pathway involving glucose transport to the branches of glycogen synthesis and glycolysis. Major control was divided between the glucose transporter and hexokinase (EC 2.7.1.1) in the glucose group. The distribution of the control was slightly shifted to hexokinase with ketones, and control at the glucose transport step was abolished in the presence of insulin. Analysis of the pathway from 3-P-glycerate to pyruvate determined that the major control was shared by enolase (EC 4.2.1.1) and pyruvate kinase (EC 2.7.1.40) in the glucose group. Addition of ketones, insulin, or the combination shifted the control to P-glycerate mutase (EC 5.4.2.1) and pyruvate kinase.

These results illustrate that the control of the metabolic flux in glucose metabolism of rat heart is not exerted by a single enzyme but variably distributed among enzymes depending upon substrate availability, hormonal stimulation, or other changes of conditions.

With the demonstration that the concentration of intracellular glucose was very low in skeletal muscle, it was first suggested that insulin might act primarily by increasing glucose transport into the cell (1). The evidence that administration of insulin increased the galactose space in eviscerated dogs (2) confirmed that a major action of insulin was to increase intracellular hexoses in insulin-sensitive tissues. It was subsequently shown that glucose transport was mediated in muscle by a carrier-facilitated process (3). In retrograde perfusion of isolated rat hearts, administration of insulin did not alter the apparent K_m of 3-O-methyl glucose transport in the forward direction but rather increased its apparent V_{max} from near 1

μmol/min/g to 12 μmol/min/g while at the same time decreasing the K_m in the reverse direction from 7 to 3 mM (4). The further finding that hearts perfused in the retrograde manner had unmeasurable [Glc]_i¹ at concentrations of extracellular glucose [Glc]_o from 2 to 16 mM contributed to the belief that [Glc]_i was very low and that, therefore, glucose transport was rate-limiting for reactions utilizing glucose (5). However, in the same study it was also observed that [Glc]_i was about 1.5 mM when hearts were perfused in the working mode, provided that extracellular glucose was elevated to the mildly hyperglycemic concentration of 16 mM and that the atrial pressure was maintained below 5 cm H₂O to limit the work-related requirement for substrate. Under very slight differences in experimental conditions, therefore, limitations imposed on a particular enzyme step were altered so that this step was no longer rate-limiting. It is, therefore, to be expected that a step that exerts a dominant effect upon flux under one set of conditions, such as insulin deprivation, may exert a quantitatively different effect upon flux under different experimental conditions (6, 7).

In contrast to the view that glucose transport is the "rate-limiting" or "pacemaker" reaction of glucose utilization, an alternative view has been expressed that many, if not all, of the enzymes of glycolysis have activities similar to the rate of glycolysis itself and that one or another of these enzymes may control flux under different conditions. Decreases of only 33% in the activity of an enzyme, P-glucosomerase, thought to operate *in vivo* very close to near-equilibrium, have been reported (8) to decrease significantly the ratio of [products] to [reactants] (Γ) measured in tissue and at the same time to cause a proportionate decrease in the rate of complex carbohydrate synthesis.

One way to deal quantitatively with the distribution of the control of the rate of flux through a metabolic pathway exerted by individual enzymatic steps or groups of enzymatic steps has been formalized in the concept of control strength (9), which

* The costs of publication of this article were defrayed in part by the payment of page charges. This article must therefore be hereby marked "advertisement" in accordance with 18 U.S.C. Section 1734 solely to indicate this fact.

[‡] Present address: Dept. of Medicine, Kitasato University School of Medicine, Sagami-hara, Kanagawa 210, Japan.

[¶] To whom correspondence should be addressed: National Institute on Alcoholism and Alcohol Abuse, 12501 Washington Ave., Rockville, MD 20852. Tel.: 301-443-4620; Fax: 301-443-0930.

¹ The abbreviations used are: Glc_i, intracellular glucose; Glc_o, extracellular glucose; Pyr, pyruvate; HK, hexokinase; UDPGase, UDP-Glc pyrophosphorylase (EC 2.7.1.1); GlycS, glycogen synthase; Plase, phosphorylase; PGK, 3-P-glycerate kinase; PGlyM and PGM, P-glycerate mutase; Eno, enolase; PK, pyruvate kinase; UDPG, UDP-Glc; Glc-6-P and G6P, glucose 6-phosphate; Fru-6-P and F6P, fructose 6-phosphate; Glc-1-P and G1P, glucose 1-phosphate; Fru-1,6-P₂, fructose 1,6-bisphosphate; Fru-2,6-P₂, fructose 2,6-bisphosphate; DHAP, dihydroxyacetone phosphate; GAP, glyceraldehyde-3-phosphate; 1,3-P₂-glycerate and 1,3DPG, 1,3-bisphosphoglycerate; 2,3-P₂-glycerate, 2,3-bisphosphoglycerate; 3-P-glycerate, 3-phosphoglycerate; 2-P-glycerate and 2PG, 2-phosphoglycerate; P-enolpyruvate and PEP, phosphoenolpyruvate; α-glycero-P, α-glycerophosphate; Glut4, glucose transporter 4; P-glucosomutase and PGM, phosphoglucosomutase; P-glucosomerase and PGI, phosphoglucosomerase; P-fructokinase, phosphofructokinase; triose-P isomerase, triose phosphate isomerase; MCA, metabolic control analysis; J, metabolic flux; C, flux control coefficient; ε, elasticity; K', equilibrium constant; Γ, ratio of products to reactants in the tissue for a given reaction. Σ denotes all ionic species of a compound; therefore, we have used [Σ...] throughout.

was subsequently termed flux control coefficient (10). Flux control coefficients (C) are defined as the fractional change in flux resulting from an infinitesimal fractional change in enzyme activity. The flux control coefficient can be determined indirectly by first calculating the elasticity (ϵ), the fractional change in the net rate of a reaction catalyzed by a particular enzyme brought about by infinitesimal fractional change in the concentration of its substrate or product (Equation 6). The degree of control exerted by each enzyme step can be determined using bottom-up analysis (9, 11). In a steady state, net rate (v) can be calculated from known kinetic and thermodynamic parameters using the Haldane equation (Equation 4) (12) to obtain the elasticity (Equation 8). The degree of control exerted by groups of enzymes can also be determined using top-down analysis (11, 13, 14). In this paper, the method of analysis is closest to that of Groen *et al.* (15). Flux can be varied in different ways: the activity of a particular enzyme may be decreased by inhibitor titration (16) or by the selection of mutants with lower activity of a specific enzyme (8); enzyme activities may be increased by addition of pure enzyme to a tissue homogenate (17) or by genetically engineered overexpression (18). Other methods to formalize analysis of flux control coefficients have also been developed (19–25).

Insulin and work were known to increase glucose transport into heart muscle (4, 26). Glucose transport was later shown to result from the translocation of Glut4 from the endoplasmic reticulum to the plasma membrane (27–31). Because insulin administration increases rapidly the number of Glut4 molecules located within the plasma membrane, glucose transport into the interior of perfused working rat heart increases as well. However, with the provision of a preferred fuel such as ketone bodies (32–34) for energy production, the transport of glucose to supply the energy requirements for the heart should decrease. We have used these two approaches: first, increasing the activity of the glucose transporter by a saturating dose of insulin (100 nM); and second, reducing the need for glucose transport by supplying 4 mM sodium D- β -hydroxybutyrate and 1 mM sodium acetoacetate as an alternative energy source. Using these strategies, we have determined for the first time in one set of data the concentrations of the intermediate metabolites, the kinetic constants of the enzymes of glucose metabolism, the values of equilibrium constants (K') for intracellular conditions of pH and free $[Mg^{2+}]$, and the flux of the pathway. With this information we have examined the effects of different physiological states on the control of flux exerted by the enzymatic steps of glycolysis and glycogen metabolism of perfused working rat heart.

EXPERIMENTAL PROCEDURES

Preparation and Perfusion of Rat Hearts

450–500-g male Wistar rats (Charles River Laboratories, Wilmington, MA) fed *ad libitum* were given 50 mg/kg of sodium pentobarbital/kg of body weight intraperitoneally (Sigma). Hearts were removed and perfused in a nonrecirculating hemoglobin-free system (35) as previously described (36). Briefly, following rapid excision, hearts were perfused in the retrograde manner (a modified Langendorff technique (37)) with modified Krebs-Henseleit buffer, pH 7.4, containing 1.2 mM P_i , free $[Mg^{2+}]$ of 0.5 mM, free $[Ca^{2+}]$ of 1.07 mM, and 10 mM glucose for ~15 min. During this period, the vena cavae and the pulmonary veins were ligated, and the pulmonary artery was catheterized to collect the effluent of the coronary sinus and the right ventricular thebesian veins. Hearts were then switched to the working mode (35) with a 10 cm H_2O preload and 80 mm Hg (108 cm H_2O) afterload for 15 min for a period of stabilization. During the succeeding 30 min, hearts were perfused with one of four buffer solutions containing: 1) 10 mM glucose; 2) 10 mM glucose plus 1 mM sodium acetoacetate and 4 mM sodium D- β -hydroxybutyrate (Sigma); 3) 10 mM glucose plus 0.05 unit/ml (~100 nM) recombinant soluble human insulin (100 units or 4 mg per ml) (Novo-Squibb, Princeton, NJ), a dose of insulin found in skeletal muscle preparations

to give maximal insulin response *in vitro* (38); or 4) 10 mM glucose plus the combination of ketone bodies and insulin. During this period, a number of parameters of cardiac function were measured as previously described (36): aortic flow, coronary flow, left ventricular dP/dt (Gould G4615-71, Valley View, OH), systolic aortic pressure (Spectramed P23X1, Oxnard CA), diastolic aortic pressure, mean aortic pressure, and left ventricular systolic pressure (Millar SPR477, Houston TX). At the end of the 30-min period, hearts were freeze-clamped to a thickness of <2 mm, submerged under liquid nitrogen, and the atrium and any adherent perfusate were removed with a dental drill. Extracts for metabolite and ion analyses were made as previously described (36), except that the extracts for Fru-2,6- P_2 analysis were prepared in 0.05 M NaOH (39) and those for glycogen were prepared by heating the tissue samples in 0.5 M NaOH at 100 °C for 15 min to destroy the glucose and solubilize the glycogen.

Enzyme Measurements

For most enzyme determinations, heart tissues were minced with scissors; homogenized at low speed on a Potter-Elvehjem glass homogenizer in 10–20 volumes of a 1:1 H_2O :glycerol mixture containing 10 mM K_2HPO_4 : KH_2PO_4 , pH 7.4, 20 mM imidazole, pH 7.4, 5 mM mercaptoethanol, 0.5 mM EDTA, and 0.02% bovine plasma albumin; and used without centrifugation. Where two substrates were involved, the K_m of the first substrate was determined in the presence of saturating concentrations of the second substrate. To preserve the interconvertible forms of glycogen synthase (EC 2.4.1.11) and phosphorylase (EC 2.4.1.1) separate homogenates were prepared in 20 mM imidazole buffer, pH 7, containing 0.5 mM dithiothreitol, 5 mM EDTA, and 20 mM KF. All of the enzyme activities were determined at 37 °C using fluorometric procedures measuring the oxidation or reduction of pyridine nucleotides (40). The basic reagent was 10 mM K_2HPO_4 : KH_2PO_4 buffer, pH 7.2, 20 mM imidazole HCl, pH 7.2, 150 mM KCl, and 5 mM $MgCl_2$; substrates, auxiliary enzymes, and cofactors were added as necessary. The kinetics of all of the enzymes of glycolysis were measured as well as the kinetics of glycogen synthase, phosphorylase, P-glucosyltransferase (EC 5.4.2.2), and glucose-6-phosphatase (EC 3.1.3.9). The analyses were conducted at high dilution by fluorometric procedures that minimize disturbing side reactions. Appropriate blanks were included to correct for nonspecific reactions. When more than one form of an enzyme might be present, the numbers represent an average value in the crude tissue; the homogenates were not purified in any manner and thus should represent as closely as possible the activity of the tissue itself. In specific instances, the reverse reactions were measured in order to do metabolic control analysis (Tables V, VI, and VII). Certain equilibrium and kinetic constants were obtained from the literature as noted in Tables IV and V (4, 41–57).

Analytical Measurements

Intra- and extracellular water spaces were measured with perfusate containing 1 $\mu Ci/ml$ 3H_2O (DuPont NEN) and 0.05 $\mu Ci/ml$ [^{14}C]mannitol (ICN Biochemicals, Costa Mesa, CA) for 5 min as previously described (36). Unless otherwise stated, glycolytic intermediates were measured using a ratio fluorometer (Optical Technology Devices, Inc., Elmsford, NY) by established methods (40). 2,3- P_2 -glycerate was measured by a fluorometric adaptation of the method of Rose and Liebowitz (58). Fru-2,6- P_2 was measured by a fluorometric adaptation of a published enzymatic method (39). cAMP was measured by radioimmunoassay (DuPont NEN). Values for metabolites, nucleotides, and cofactors are given as micromoles per milliliter of intracellular water; to convert micromoles per gram wet weight, to micromoles per milliliter of intracellular water the values were multiplied by 2.88 as determined by space measurements.

Metabolic Flux

The rate of glucose utilization was determined with high pressure liquid chromatography purified [2-^3H]glucose (DuPont NEN). Tritiated glucose (0.75 mCi) was added to 200 μl of perfusate (375 $\mu Ci/mmol$). The coronary outflow was collected during a timed interval, usually 2 min. The phosphorylated intermediates and glucose were removed by passing the sample over formate and borate Dowex 50 columns in sequence (59). The tritiated water remaining was a measure of the flux through P-glucosyltransferase; no correction was made for incomplete equilibration at this step (60). The removal of the labeled glucose and intermediates was confirmed by evaporating a portion of the effluent from the column; less than 0.1% of the counts remained. The rates of glycogenolysis or glycogenesis were calculated from the Δ glycogen as glucosyl units from the end of the initial perfusion of 15 min to the end of the 30-min experimental treatment (Fig. 1).

Calculations

Statistical analyses of the significance of the difference between means were calculated using a Mann-Whitney U test (Stat-View-4, Abacus Concepts, Inc., Berkeley, CA). Cytoplasmic $[P_i]$ was determined by ^{31}P NMR; the cytoplasmic pH was taken from the shift of the intracellular P_i from phosphocreatine,² and the cytoplasmic free $[\text{Mg}^{2+}]$ was calculated using the measured $[\Sigma\text{citrate}]/[\Sigma\text{isocitrate}]$ ratio (61) (Table II). Cytoplasmic $[\Sigma\text{ATP}]/[\Sigma\text{ADP}]$ ratios were calculated as previously described (36). All equilibrium constants were corrected, where appropriate, for the pH and free $[\text{Mg}^{2+}]$ by methods previously described (62) using the equilibrium constants that had been determined under conditions approximating the intracellular environment. The values for $[\text{GAP}]$, $[\text{Fru-1,6-P}_2]$, and $[\text{1,3-P}_2\text{-glycerate}]$ are calculated from the equilibrium constant of triose-P isomerase (EC 5.3.1.1), aldolase (EC 4.1.2.13), and 3-P-glycerate kinase (EC 2.7.2.3) using the individual values of measured metabolites. All other calculations were made correcting for intra- and extracellular volumes (36). Changes in metabolite levels are presented as proportionate change, which is equal to $n \times (\text{experimental value/control values})^n$; $n = 1$ when the experimental > control, and $n = -1$ when the experimental < control, thus assigning equal value to increases and decreases (63). Cardiac hydraulic work was calculated as follows,

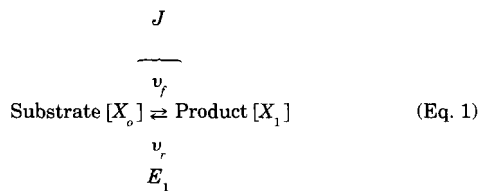
$$\text{cardiac hydraulic work (J/min/g wet weight)} =$$

$$\frac{\text{cardiac output (ml/min)} \times \text{aortic pressure (mm Hg)}}{\text{left ventricle weight (g wet weight)}} \times \frac{101,325 \text{ (Nm}^{-2}\text{)}}{760 \text{ (mm Hg)}}$$

where 1 atm = 760 mm Hg = 101,325 newtons/m² (Nm⁻²).

Method of Calculation of Metabolic Control Parameters

A variable property of a system will respond to a variation of some parameter; for example, metabolic flux will respond to changes in enzyme activity or metabolite concentration. A simple model is shown below.



where i is number of the step, 1– n (in this model, $i = 1$); $[X]$ is concentration of the metabolite ($[X_o] = [X_{i-1}]$, concentration of the substrate, $[S]$; $[X_i] = [X]$, concentration of the product, $[P]$); v_f is rate of conversion of substrate to product; v_r is rate of conversion of product to substrate; v is net rate of an individual enzyme step; J is flux through the pathway of the system (in this one-step model $J = v = v_f - v_r$); and E_i is enzyme catalyzing step i denoted by the subscript.

1. Michaelis-Menten Initial Rate Equation with One Substrate or One Product (64)

$$v_f = V_{\max F}/(1 + K_{m,S}/[S]) \quad v_r = V_{\max R}/(1 + K_{m,P}/[P]) \quad (\text{Eq. 2})$$

where $K_{m,S}$ is Michaelis constant (K_m) of $[S]$, forward direction; $K_{m,P}$ is Michaelis constant (K_m) of $[P]$, reverse direction; $V_{\max F}$ is maximum velocity of an enzyme step in the forward direction; and $V_{\max R}$ is maximum velocity of an enzyme step in the reverse direction.

2. Law of Microscopic Reversibility, Haldane Relationship, and Steady-state Rate Equation with One Substrate and One Product, Assuming Michaelis-Menten Kinetics (12)

At equilibrium,

$$v_f = v_r \text{ and } v = 0, \quad K' = (V_{\max F} \times K_{m,P})/(V_{\max R} \times K_{m,S}) \quad (\text{Eq. 3})$$

$$v = \frac{V_{\max F}/K_{m,S} ([S] - [P]/K')}{1 + [S]/K_{m,S} + [P]/K_{m,P}} = \frac{V_{\max F}[S]/K_{m,S} - V_{\max R}[P]/K_{m,P}}{1 + [S]/K_{m,S} + [P]/K_{m,P}} \quad (\text{Eq. 4})$$

where K' is the equilibrium ratio of $[P]$ to $[S]$ determined *in vitro* under specified conditions.

3. Flux Control Coefficient

The flux control coefficient (C) is the fractional change in the flux of the system ($\delta J/J$) that results from an infinitesimal fractional change in

the rate of enzyme catalytic activity ($\delta e/e$) in step i .

$$C_{E_i}^J = \lim_{\delta e_i \rightarrow 0} \frac{\delta J/J}{\delta e_i/e_i} = \frac{\delta J}{\delta e_i} \cdot \frac{e_i}{J} \quad (\text{Eq. 5})$$

C can be calculated in two ways. In the direct method, flux is measured and the enzyme concentration is titrated by the addition of enzyme or inhibitors and does not require the calculation of elasticities (17, 65–67). In the indirect method, elasticities of the steps must first be determined (see step 4 below), and C can be calculated from these data (9, 15, 19, 20).

4. Elasticity

The elasticity (ϵ) of an enzyme is the fractional change in the net rate for an individual reaction ($\delta v_i/v_i$), caused by an infinitesimal fractional change of metabolite concentration ($\delta [X]/[X]$) in step i . In this model, X_{i-1} is the substrate and X_i is the product of E_i (for review see Ref. 23).

$$\epsilon_{X_{i-1}(\text{substrate})}^{E_i} = \lim_{\delta [S] \rightarrow 0} \frac{\delta v_i/v_i}{\delta [S]/[S]} = \frac{\delta v_i}{\delta [S]} \cdot \frac{[S]}{v_i} \quad (\text{Eq. 6})$$

$$\epsilon_{X_i(\text{product})}^{E_i} = \lim_{\delta [P] \rightarrow 0} \frac{\delta v_i/v_i}{\delta [P]/[P]} = \frac{\delta v_i}{\delta [P]} \cdot \frac{[P]}{v_i}$$

4a. Calculation of ϵ from Change in Flux

$$\epsilon_{\text{substrate}}^{E_i} \approx \Delta \ln v / \Delta \ln [S], \quad \epsilon_{\text{product}}^{E_i} \approx \Delta \ln v / \Delta \ln [P] \quad (\text{Eq. 7})$$

This equation can be regarded as the finite approximation to the elasticity definition. To calculate ϵ by this method one needs measurements of net rate (Table I) and substrate concentrations (Table II). The above relationship (Equation 7) allows estimation of the block elasticity if the following conditions are met: 1) the flux (J) through a block of the reaction is equal to the net rate (v) of the step, 2) the flux is dependent on the concentration of only one metabolite outside of the block, and 3) the flux is changed by a perturbation in some other part of the metabolic pathway that causes a change in $[S]$.

4b. Calculation of ϵ from Kinetic Data—If a steady state prevails and if the tissue reactions follow Michaelis-Menten kinetics, the net rate of the steady-state equation (Equation 4) can be substituted into Equation 6. The derivative of Equation 6 yields Equation 8. To calculate ϵ from the kinetic parameters of the enzymes one needs the following: (a) the K_m and V_{\max} of forward and backward direction of each enzyme involved and the K_a and K_i of other substances that alter the kinetic parameters (Table V); (b) the concentration of the substrates ($[S]$) and products ($[P]$) of each reaction (Table II) and the ratio of the products to reactants in the tissue (Γ) (Table IV); (c) the equilibrium constant (K') of the reaction under appropriate conditions of temperature, ionic strength, pH, and free $[\text{Mg}^{2+}]$ under which the reactions are occurring (Table IV); and (d) the architecture of the pathway, that is whether it is linear or branched, and the ratio of fluxes at the branch points (Table I and Equation 11).

$$\epsilon_S^{E_i} = \frac{1}{1 - \Gamma/K'_{E_i}} - \frac{[S]/K_{m,S(E_i)}}{1 + [S]/K_{m,S(E_i)} + [P]/K_{m,P(E_i)}} = \frac{1}{1 - \Gamma/K'_{E_i}} - \frac{v_{f,E_i}}{V_{\max F,E_i}} \quad (\text{Eq. 8})$$

$$\epsilon_P^{E_i} = \frac{-\Gamma/K'_{E_i}}{1 - \Gamma/K'_{E_i}} - \frac{[P]/K_{m,P(E_i)}}{1 + [S]/K_{m,S(E_i)} + [P]/K_{m,P(E_i)}} = \frac{-\Gamma/K'_{E_i}}{1 - \Gamma/K'_{E_i}} - \frac{v_{r,E_i}}{V_{\max R,E_i}}$$

$$v_r/v_f = \Gamma/K'$$

The expressions $v_f/V_{\max F}$ and $v_r/V_{\max R}$ represent the fractional saturation of the enzyme with $[S]$ and $[P]$, respectively (to the extent that $K_{m,S}$ and $K_{m,P}$ approximate true dissociation constants).

5. Summation Theorem

The sum of all flux control coefficients of any chosen linear flux (J) for all of the n enzymes in a metabolic sequence is 1.

$$\sum_{i=1}^n C_{E_i}^J = 1 \quad (\text{Eq. 9})$$

where n is the number of steps in the sequence chosen.

6. Connectivity Theorem

The flux control coefficients are related to the elasticities of all en-

² K. Clarke and C. Keon, unpublished observations.

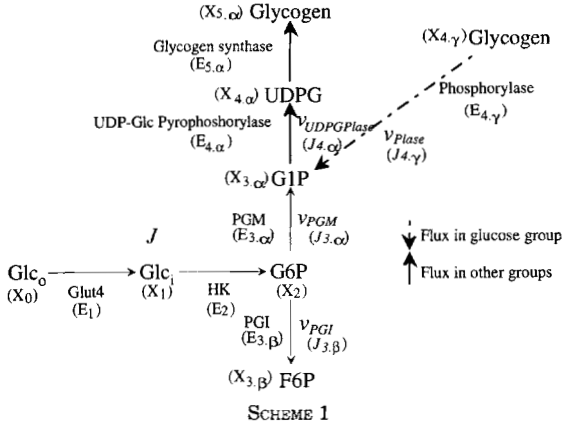
zymes that respond to the concentration of a single metabolite [X].

$$\sum_{i=z}^n C_{E_i}^J \epsilon_X^{E_i} = 0 \quad (\text{Eq. 10})$$

7. Branch Point Theorem

At a branch point under steady-state conditions, the sum of the flux control coefficients of enzymes in the branches is equal to the ratio of flux through the branches.

$$\frac{\sum C_{i,\alpha}^J}{\sum C_{i,\beta}^J} = \frac{v_{i,\alpha}}{v_{i,\beta}}, \quad -v_{i,\alpha} (\sum C_{i,\beta}^J) + v_{i,\beta} (\sum C_{i,\alpha}^J) = 0$$



In Scheme 1, branch point at Glc-6-P, the equation would be

$$\sum_{i=3}^n C_{i,\alpha}^J / C_{i,\beta}^J = v_{3,\alpha} / v_{3,\beta},$$

for the glucose group specifically,

$$(C_{3,\alpha}^J + C_{4,\gamma}^J) / C_{3,\beta}^J = v_{3,\alpha} / v_{3,\beta}, \quad (\text{Eq. 11})$$

and for the other groups,

$$(C_{3,\alpha}^J + C_{4,\alpha}^J + C_{5,\alpha}^J) / C_{3,\beta}^J = v_{3,\alpha} / v_{3,\beta},$$

where α , β , and γ are branched steps in step i .

8. Matrix Method of Control Analysis (11, 68)

$$E \cdot C = M, \quad C = E^{-1} \cdot M \quad (\text{Eq. 12})$$

where E is the elasticity matrix; C is the flux control coefficient matrix; and M is the matrix that defines the relationships between the elements of E and the flux control coefficients in C .

Application of Metabolic Control Analysis

We performed "bottom-up" (11, 23) and "top-down" (11, 13, 14) analyses. Bottom-up analysis considers individual enzyme steps with regard to their elasticities. In contrast, top-down analysis considers groups of enzymes, using group elasticities. In our applications, the differences between top-down and bottom-up analyses are: 1) top-down analysis applies to the whole of glucose metabolism, i.e. the effects of reactions beyond the block analyzed are included; 2) because different block elasticities were derived by taking different pairs of the experimental sets, there is a single result from the top-down method, which is an approximate average over the states considered. Fuller explanations as models are given below.

1. Model of Bottom-up Analysis

ϵ was determined for the individual enzyme steps of the branched pathway from glucose transport to glycogen metabolism and P-glucosylomerase step (Scheme 1) and also for the steps of the terminal linear pathway of glycolysis from 3-P-glycerate kinase to pyruvate kinase (Scheme 2) using the data from Tables II-V. For each pathway analyzed, $\sum C^J = 1$.

1A. Glucose Transport to the Branches of Glycogen Metabolism and P-glucosylomerase Step—Scheme 1 is a model of glycogen metabolism and illustrates both glycogenolysis and glycogen synthesis. The activity of Glc-6-P dehydrogenase (EC 1.1.1.49) in the heart was 10^2 - 10^3 lower than that of P-glucosylomerase and P-glucosylomerase (Table V), and the

oxidative portion of the hexose monophosphate pathway was, therefore, ignored. In the presence of glucose alone, there was net phosphorolysis of glycogen (shown as *dashed arrow*) and the net rate of the P-glucosylomerase reaction was in the direction of Glc-6-P formation; $J_{3,\alpha} \approx J_{4,\gamma}$, $J_{4,\alpha} \approx 0$. The value of glycogen synthase was not considered. In the presence of ketones and/or insulin, there was net glycogen synthesis, and the net rate of the P-glucosylomerase reaction was in the direction of Glc-1-P formation (shown as a *solid arrow*); $J_{3,\alpha} \approx J_{4,\alpha}$, $J_{4,\gamma} \approx 0$. In these cases, phosphorolysis was not considered. Elasticities were calculated using kinetic data (Equation 8).

$$\epsilon_{Glc_1}^{Glut4} = \frac{-[Glc_1] / [Glc_0]}{1 - [Glc_1] / [Glc_0]} \cdot \frac{K'_{Glut4}}{K'_{Glut4}} - \frac{v_r}{V_{maxR}} \quad (\text{Eq. 13})$$

$$\epsilon_{Glc_1}^{HK} = \frac{1}{1 - [G6P] / [Glc_1]} - \frac{[Glc_1] / K_{m,Glc_1(HK)}}{1 + [Glc_1] / K_{m,Glc_1(HK)} + [G6P] / K_{m,G6P(HK)}}$$

$$\epsilon_{G6P}^{HK} = \frac{-[G6P] / [Glc_1]}{1 - [G6P] / [Glc_1]} \cdot \frac{K'_{HK}}{K'_{HK}} - \frac{[G6P] / K_{m,G6P(HK)}}{1 + [Glc_1] / K_{m,Glc_1(HK)} + [G6P] / K_{m,G6P(HK)}}$$

$$\epsilon_{G6P}^{PGM} = \frac{1}{1 - [G1P] / [G6P]} - \frac{[G6P] / K_{m,G6P(PGM)}}{1 + [G6P] / K_{m,G6P(PGM)} + [G1P] / K_{m,G1P(PGM)}}$$

$$\epsilon_{G1P}^{PGM} = \frac{-[G1P] / [G6P]}{1 - [G1P] / [G6P]} \cdot \frac{K'_{PGM}}{K'_{PGM}} - \frac{[G1P] / K_{m,G1P(PGM)}}{1 + [G6P] / K_{m,G6P(PGM)} + [G1P] / K_{m,G1P(PGM)}}$$

$$\epsilon_{G6P}^{PGI} = \frac{1}{1 - [F6P] / [G6P]} - \frac{[G6P] / K_{m,G6P(PGI)}}{1 + [G6P] / K_{m,G6P(PGI)} + [F6P] / K_{m,F6P(PGI)}}$$

$$\epsilon_{G1P}^{UDPGPlase} = 100, \quad \epsilon_{UDPG}^{UDPGPlase} = -100$$

$$\epsilon_{UDPG}^{GlycS} = 1 - \frac{[UDPG]}{[UDPG] + K_{m,UDPG(UDPGPlase)}} = \frac{K_{m,UDPG(UDPGPlase)}}{K_{m,UDPG(UDPGPlase)} + [UDPG]}$$

Calculation of the flux control coefficients in the glucose group is as follows.

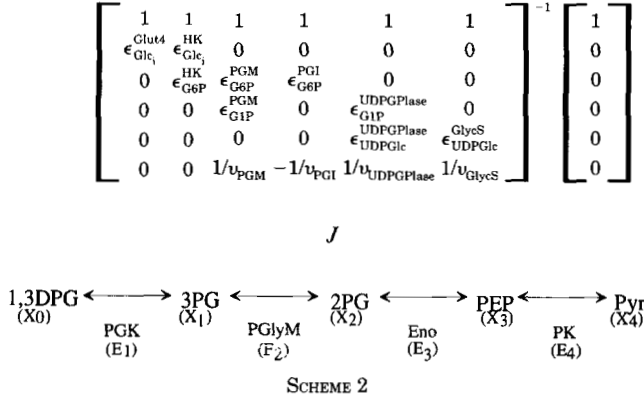
$$\begin{aligned} C_{Glut4}^J + C_{HK}^J + C_{PGM}^J + C_{PGI}^J + C_{Plase}^J &= 1 \\ C_{Glut4}^J \epsilon_{Glc_1}^{Glut4} + C_{HK}^J \epsilon_{Glc_1}^{HK} &= 0 \\ C_{HK}^J \epsilon_{G6P}^{HK} + C_{PGM}^J \epsilon_{G6P}^{PGM} + C_{PGI}^J \epsilon_{G6P}^{PGI} &= 0 \\ C_{PGM}^J \epsilon_{G1P}^{PGM} + C_{Plase}^J \epsilon_{G1P}^{Plase} &= 0 \\ -C_{PGM}^J / v_{PGM} + C_{PGI}^J / v_{PGI} + C_{Plase}^J / v_{Plase} &= 0 \end{aligned} \quad (\text{Eq. 14})$$

$$\begin{bmatrix} C_{Glut4}^J \\ C_{HK}^J \\ C_{PGM}^J \\ C_{PGI}^J \\ C_{Plase}^J \end{bmatrix} = \begin{bmatrix} 1 & 1 & 1 & 1 & 1 \\ \epsilon_{Glc_1}^{Glut4} & \epsilon_{Glc_1}^{HK} & 0 & 0 & 0 \\ 0 & \epsilon_{G6P}^{HK} & \epsilon_{G6P}^{PGM} & \epsilon_{G6P}^{PGI} & 0 \\ 0 & 0 & \epsilon_{G1P}^{PGM} & 0 & \epsilon_{G1P}^{Plase} \\ 0 & 0 & -1/v_{PGM} & 1/v_{PGI} & 1/v_{Plase} \end{bmatrix}^{-1} \begin{bmatrix} 1 \\ 0 \\ 0 \\ 0 \\ 0 \end{bmatrix} \quad (\text{Eq. 15})$$

Calculation of the flux control coefficients in the ketones, insulin, and ketones plus insulin groups is as follows.

$$\begin{aligned} C_{Glut4}^J + C_{HK}^J + C_{PGM}^J + C_{PGI}^J + C_{UDPGPlase}^J + C_{GlycS}^J &= 1 \\ C_{Glut4}^J \epsilon_{Glc_1}^{Glut4} + C_{HK}^J \epsilon_{Glc_1}^{HK} &= 0 \\ C_{HK}^J \epsilon_{G6P}^{HK} + C_{PGM}^J \epsilon_{G6P}^{PGM} + C_{PGI}^J \epsilon_{G6P}^{PGI} &= 0 \\ C_{PGM}^J \epsilon_{G1P}^{PGM} + C_{UDPGPlase}^J \epsilon_{G1P}^{UDPGPlase} &= 0 \\ C_{UDPGPlase}^J \epsilon_{UDPG}^{UDPGPlase} + C_{GlycS}^J \epsilon_{UDPG}^{GlycS} &= 0 \\ C_{PGM}^J / v_{PGM} - C_{PGI}^J / v_{PGI} + C_{UDPGPlase}^J / v_{UDPGPlase} + C_{GlycS}^J / v_{GlycS} &= 0 \end{aligned} \quad (\text{Eq. 16})$$

$$\begin{bmatrix} C_{\text{GluT4}}^J \\ C_{\text{HK}}^J \\ C_{\text{PGM}}^J \\ C_{\text{PGI}}^J \\ C_{\text{UDPGase}}^J \\ C_{\text{GlycS}}^J \end{bmatrix} = \begin{bmatrix} 1 & 1 & 1 & 1 & 1 & 1 \\ \epsilon_{\text{Glc}_i}^{\text{GluT4}} & \epsilon_{\text{Glc}_i}^{\text{HK}} & 0 & 0 & 0 & 0 \\ 0 & \epsilon_{\text{G6P}}^{\text{HK}} & \epsilon_{\text{G6P}}^{\text{PGM}} & \epsilon_{\text{G6P}}^{\text{PGI}} & 0 & 0 \\ 0 & 0 & \epsilon_{\text{G1P}}^{\text{PGM}} & 0 & \epsilon_{\text{G1P}}^{\text{UDPGase}} & 0 \\ 0 & 0 & 0 & 0 & \epsilon_{\text{UDPGase}}^{\text{UDPGase}} & \epsilon_{\text{UDPGase}}^{\text{GlycS}} \\ 0 & 0 & 1/\nu_{\text{PGM}} & -1/\nu_{\text{PGI}} & 1/\nu_{\text{UDPGase}} & 1/\nu_{\text{GlycS}} \end{bmatrix}^{-1} \begin{bmatrix} 1 \\ 0 \\ 0 \\ 0 \\ 0 \\ 0 \end{bmatrix} \quad (\text{Eq. 17})$$



1B. Terminal Linear Pathway in Glycolysis (Scheme 2)

$$\epsilon_{3\text{PG}}^{\text{PGK}} = \frac{-\frac{[3\text{PG}]}{[1,3\text{DPG}]} / K'_{\text{PGK}}}{1 - \frac{[3\text{PG}]}{[1,3\text{DPG}]} / K'_{\text{PGK}}}$$

$$\epsilon_{3\text{PG}}^{\text{PGlyM}} = \frac{1}{1 - \frac{[2\text{PG}]}{[3\text{PG}]} / K'_{\text{PGlyM}}} - \frac{[3\text{PG}]/K_{m,3\text{PG}(\text{PGK})}}{1 + [1,3\text{DPG}]/K_{m,1,3\text{DPG}(\text{PGK})} + [3\text{PG}]/K_{m,3\text{PG}(\text{PGK})}}$$

$$\epsilon_{2\text{PG}}^{\text{PGlyM}} = \frac{\frac{[2\text{PG}]}{[3\text{PG}]} / K'_{\text{PGlyM}}}{1 - \frac{[2\text{PG}]}{[3\text{PG}]} / K'_{\text{PGlyM}}} - \frac{[2\text{PG}]/K_{m,2\text{PG}(\text{PGlyM})}}{1 + [3\text{PG}]/K_{m,3\text{PG}(\text{PGlyM})} + [2\text{PG}]/K_{m,2\text{PG}(\text{PGlyM})}}$$

$$\epsilon_{2\text{PG}}^{\text{Eno}} = \frac{1}{1 - \frac{[\text{PEP}]}{[2\text{PG}]} / K'_{\text{Eno}}} - \frac{[2\text{PG}]/K_{m,2\text{PG}(\text{Eno})}}{1 + [2\text{PG}]/K_{m,2\text{PG}(\text{Eno})} + [\text{PEP}]/K_{m,\text{PEP}(\text{Eno})}}$$

$$\epsilon_{\text{PEP}}^{\text{Eno}} = \frac{\frac{[\text{PEP}]}{[2\text{PG}]} / K'_{\text{Eno}}}{1 - \frac{[\text{PEP}]}{[2\text{PG}]} / K'_{\text{Eno}}} - \frac{[\text{PEP}]/K_{m,\text{PEP}(\text{Eno})}}{1 + [2\text{PG}]/K_{m,2\text{PG}(\text{Eno})} + [\text{PEP}]/K_{m,\text{PEP}(\text{Eno})}}$$

$$\epsilon_{\text{PEP}}^{\text{PK}} = \frac{1}{1 - \frac{[\text{Pyr}]}{[\text{PEP}]} / K'_{\text{PK}}} - \frac{[\text{PEP}]/K_{m,\text{PEP}(\text{PK})}}{1 + [\text{PEP}]/K_{m,\text{PEP}(\text{PK})} + [\text{Pyr}]/K_{m,\text{Pyr}(\text{PK})}} \quad (\text{Eq. 18})$$

$$C_{\text{PGK}}^J + C_{\text{PGlyM}}^J + C_{\text{Eno}}^J + C_{\text{PK}}^J = 1$$

$$C_{\text{PGK}}^J \epsilon_{3\text{PG}}^{\text{PGK}} + C_{\text{PGlyM}}^J \epsilon_{3\text{PG}}^{\text{PGlyM}} = 0 \quad (\text{Eq. 19})$$

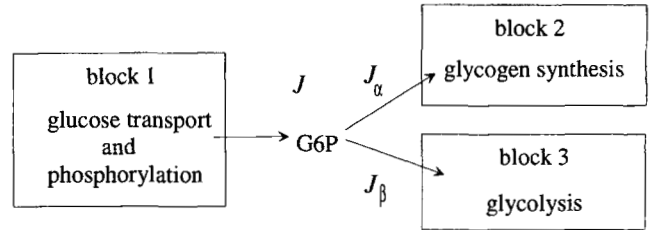
$$C_{\text{PGlyM}}^J \epsilon_{2\text{PG}}^{\text{PGlyM}} + C_{\text{Eno}}^J \epsilon_{2\text{PG}}^{\text{Eno}} = 0$$

$$C_{\text{Eno}}^J \epsilon_{\text{PEP}}^{\text{Eno}} + C_{\text{PK}}^J \epsilon_{\text{PEP}}^{\text{PK}} = 0$$

$$\begin{bmatrix} C_{\text{PGK}}^J \\ C_{\text{PGlyM}}^J \\ C_{\text{Eno}}^J \\ C_{\text{PK}}^J \end{bmatrix} = \begin{bmatrix} 1 & 1 & 1 & 1 \\ \epsilon_{3\text{PG}}^{\text{PGK}} & \epsilon_{3\text{PG}}^{\text{PGlyM}} & 0 & 0 \\ 0 & \epsilon_{2\text{PG}}^{\text{PGlyM}} & \epsilon_{2\text{PG}}^{\text{Eno}} & 0 \\ 0 & 0 & \epsilon_{\text{PEP}}^{\text{Eno}} & \epsilon_{\text{PEP}}^{\text{PK}} \end{bmatrix}^{-1} \begin{bmatrix} 1 \\ 0 \\ 0 \\ 0 \end{bmatrix} \quad (\text{Eq. 20})$$

Whenever Γ/K' was ≥ 1 we assumed an equilibrium state, and where ϵ_p and ϵ_s approached negative and positive infinity, respectively, the numbers -100 or 100 were assigned to solve the equations using matrix

algebra. In the glucose and ketones groups, Γ for the glucose transport step was far from equilibrium; intracellular glucose was low but several times higher than the K_m of hexokinase for glucose, so the use of glucose by hexokinase would be favored. The elasticity calculation does include a contribution for the reversibility in the term involving the disequilibrium ratio, but the smaller contribution from the fractional saturation of the carrier ($\nu_i/\nu_{\text{max},i}$) approaches 0 in the glucose and glucose plus ketones groups where $[\text{Glc}_i] \gg [\text{Glc}_i]$ and has been taken to be 1 in the presence of insulin where $[\text{Glc}_i] \approx [\text{Glc}_i]$. The reaction of UDP-Glc pyrophosphorylase was assumed to be in a state of near-equilibrium, and the elasticities were assigned as described above. The reaction of glycogen synthase was taken to be irreversible (Table IV). The net rate of glycogen synthase was assigned the calculated ν_i from the Michaelis-Menten equation (Equation 4) and substituted in Equation 6, and the derivative was taken.



SCHEME 3

2. Model of Top-down Analysis

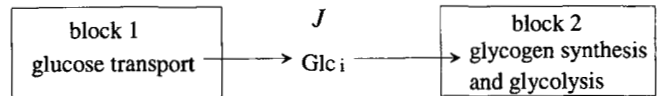
Two forms of top-down analysis were performed considering all of glucose metabolism as a single system (Schemes 3 and 4).

2A. Glc-6-P as Intermediate Metabolite (Scheme 3)

$$\begin{aligned} \epsilon_{\text{G6P}}^1 &\approx \Delta \ln J / \Delta \ln [\text{G6P}], \\ \epsilon_{\text{G6P}}^2 &\approx \Delta \ln J_\alpha / \Delta \ln [\text{G6P}], \\ \epsilon_{\text{G6P}}^3 &\approx \Delta \ln J_\beta / \Delta \ln [\text{G6P}] \end{aligned} \quad (\text{Eq. 21})$$

$$\begin{bmatrix} C_1^J \\ C_2^J \\ C_3^J \end{bmatrix} = \begin{bmatrix} 1 & 1 & 1 \\ \epsilon_{\text{G6P}}^1 & \epsilon_{\text{G6P}}^2 & \epsilon_{\text{G6P}}^3 \\ 0 & 1/J_\alpha & -1/J_\beta \end{bmatrix}^{-1} \begin{bmatrix} 1 \\ 0 \\ 0 \end{bmatrix} \quad (\text{Eq. 22})$$

2B. Intracellular Glucose as Intermediate Metabolite (Scheme 4)



SCHEME 4

$$\epsilon_{\text{Glc}_i}^1 = \epsilon_{\text{Glc}_i}^{\text{GluT4}} \quad (\text{Eq. 13}), \quad \epsilon_{\text{Glc}_i}^2 \approx \Delta \ln J / \Delta \ln [\text{Glc}_i] \quad (\text{Eq. 23})$$

$$\begin{bmatrix} C_1^J \\ C_2^J \end{bmatrix} = \begin{bmatrix} 1 & 1 \\ \epsilon_{\text{Glc}_i}^1 & \epsilon_{\text{Glc}_i}^2 \end{bmatrix}^{-1} \begin{bmatrix} 1 \\ 0 \end{bmatrix} \quad (\text{Eq. 24})$$

In the first case, centering on Glc-6-P, glucose transport and phosphorylation was taken as block 1, glycogen synthesis as block 2, and glycolysis as block 3. Because insulin markedly increases the V_{max} of the glucose transporter and thus ϵ_{G6P}^1 (Equation 21), it is inappropriate to calculate a flux control coefficient for block 1 from a comparison of changes of flux induced by addition of insulin to glucose-perfused hearts. We may, however, compare changes of flux induced by addition of ketones to glucose-perfused hearts (Equation 22, column 1) and by the addition of insulin to hearts perfused with glucose plus ketones in blocks 2 and 3 (Equation 22, columns 2 and 3). In this case, insulin was regarded as perturbing block 1, allowing calculation of the elasticity of blocks 2 and 3; and ketones were regarded as perturbing block 3, allowing calculation of blocks 1 and 2. Where an elasticity could be calculated in more than one way, an error analysis was performed to identify the more reliable value.

RESULTS

Cardiac hydraulic work was significantly elevated from 0.30 to 0.37 and 0.34 J/min/g wet weight, in the presence of ketones

or insulin, respectively, but was not altered in the presence of both effectors (Table I). The increase in cardiac hydraulic work was primarily the result of an increase in systolic aortic pressure from 90.5 to 96.0 mm Hg. In the presence of glucose alone, glycogen decreased at a rate of 0.46 μmol of glucosyl units/min/ml of intracellular water. After the addition of ketones, insulin, or the combination, glycogen was synthesized at the rates of 0.67, 2.6, and 2.5 μmol of glucosyl units/min/ml of intracellular water, respectively (Table I). In the presence of insulin, the production of $^3\text{H}_2\text{O}$ from $[2\text{-}^3\text{H}]\text{glucose}$ increased from 4.58 to 6.36 $\mu\text{mol}/\text{min}/\text{ml}$ of intracellular water but decreased to 2.36 in the presence of ketones. When glycogen synthesis or breakdown was combined with the measurement of $^3\text{H}_2\text{O}$ release at the P-glucosomerase step, net glycolytic flux in hearts perfused with glucose alone was 5.04 $\mu\text{mol}/\text{min}/\text{ml}$ of intracellular water in glucose-perfused hearts (Table I). As expected, net glycolytic flux decreased 3.0-fold on provision of the alternative substrate of ketone bodies and 2.3-fold on addition of insulin plus ketones; the addition of insulin alone caused no statistically significant change. The production of L-lactate at 10 cm H_2O right atrial pressure accounted for only 0.3% of the glucose use in the glucose group and increased to 1, 7, and 0.7% in the ketones, insulin, and ketones plus insulin groups, respectively.

$[\text{Glc}_i]$ was 1.91 $\mu\text{mol}/\text{ml}$ of intracellular water (Table II) in these working hearts, far above the K_m of 0.072 mM for the hexokinase reaction (Table V). Decreasing the requirement for glucose by substituting ketone bodies for pyruvate as the major provider of NADH for electron transport increased $[\text{Glc}_i]$ to 3.4 $\mu\text{mol}/\text{ml}$ of intracellular water, whereas the addition of 100 nM insulin equilibrated $[\text{Glc}_i]$ with $[\text{Glc}_o]$. $[\text{Glc-6-P}]$ was 0.17 and $[\text{Fru-6-P}]$ was 0.04 $\mu\text{mol}/\text{ml}$ of intracellular water in hearts perfused with glucose alone. The increase in $[\text{Glc-6-P}]$ was 3.5-fold with ketones, 7.5-fold with insulin, and 10-fold with the combination (Table II, Fig. 1). However, equilibrium was maintained in the P-glucosomerase reaction; Γ/K' was near 1 under all conditions studied (Table IV). $[\text{Glc-1-P}]$ was 0.02 $\mu\text{mol}/\text{ml}$ of intracellular water and increased slightly in the presence of ketones or insulin, but it increased 10-fold in the ketones plus insulin group, near-equilibrium for the P-glucosomerase reaction (Table IV).

$[\text{Glycogen}]$ was 35.3 μmol of glucosyl units/ml of intracellular water (Table II, Fig. 1) at the end of the 15-min stabilization period. After 30 min of perfusion in the experimental period, $[\text{glycogen}]$ decreased to 21.4 μmol of glucosyl units/ml of intracellular water in the glucose group and increased to 55.5 in the presence of ketones, 112 in the presence of insulin, and 109 in

TABLE I
Physiological and metabolic parameters in perfused working rat hearts

Except for cardiac hydraulic work, the data are given as $\mu\text{mol}/\text{min}/\text{ml}$ of intracellular water \pm S.E. with the number of observations given in parentheses. Significant differences from glucose alone for lines 1 and 2 are indicated. Calculations in lines 3 and 4 are average values; standard error is based on the combination of error formula for the sum or difference of two figures, i.e. for $z = x - y$: $S_z = \sqrt{(S_x)^2 + (S_y)^2}$ where S_z is the standard error in z , etc. Hydraulic work and $^3\text{H}_2\text{O}$ production from $[2\text{-}^3\text{H}]\text{glucose}$ were determined as described under "Experimental Procedures."

	Glucose	Glucose + ketones	Glucose + insulin	Glucose + ketones + insulin
Hydraulic work (J/min/g wet weight)	0.30 \pm 0.01 (8)	0.37 \pm 0.01 ^a (8)	0.34 \pm 0.01 ^a (4)	0.32 \pm 0.01 (4)
$^3\text{H}_2\text{O}$ production from $[2\text{-}^3\text{H}]\text{glucose}$	4.58 \pm 0.75 (3)	2.37 \pm 0.69 ^a (3)	6.36 \pm 0.32 ^a (3)	4.66 \pm 0.5 (3)
Glycogen synthesis	-0.463 \pm 0.12	0.673 \pm 0.14	2.56 \pm 0.43	2.46 \pm 0.15
Net glycolytic flux through P-glucosomerase	5.04 \pm 0.76	1.70 \pm 0.70	3.80 \pm 0.53	2.20 \pm 0.52
L-Lactate exiting heart	0.030 (2)	0.050 (2)	0.400 (2)	0.066 (2)

^a $p < 0.05$, Mann-Whitney U test.

TABLE II
Metabolite concentrations in perfused working rat hearts

Metabolites in extracts from freeze-clamped hearts were measured as described under "Experimental Procedures" and given as means \pm S.E. in $\mu\text{mol}/\text{ml}$ of intracellular water. The numbers of observations in each group are as follows: glucose = 8, ketones = 3, insulin = 3, and ketones and insulin = 4, except for the following: pyruvate = 4, 5, 7, and 7; 2-P-glycerate and P-enolpyruvate = 5, 3, 3, and 3; and glycogen and Fru-2,6-P₂ = 3, 2, 2, and 3, respectively. Significant differences from glucose-perfused hearts are indicated. When there were only two samples, S.E. = range/ n .

Metabolite	Glucose	Glucose + ketones	Glucose + insulin	Glucose + ketones + insulin
Glycogen ^a	21.4 \pm 1.62	55.5 \pm 2.95 ^b	112 \pm 12.4 ^b	109 \pm 3.31 ^b
Glc-1-P	0.020 \pm 0.004	0.035 \pm 0.020	0.057 \pm 0.012	0.198 \pm 0.077 ^b
Glc-1,6-P ₂	0.007 \pm 0.000	0.008 \pm 0.002	0.013 \pm 0.003 ^b	0.009 \pm 0.001
Glc-6-P	0.169 \pm 0.010	0.612 \pm 0.082 ^b	1.268 \pm 0.020 ^b	1.626 \pm 0.508 ^b
Glc _i	1.91 \pm 0.503	3.40 \pm 1.12	11.5 \pm 1.09 ^b	9.94 \pm 0.712 ^b
Fru-6-P	0.041 \pm 0.005	0.155 \pm 0.026 ^b	0.342 \pm 0.003 ^b	0.321 \pm 0.053 ^b
Fru-1,6-P ₂ (total)	0.035 \pm 0.003	0.016 \pm 0.000 ^b	0.040 \pm 0.002	0.033 \pm 0.005
(calculated, $\times 10^3$)	0.678 \pm 0.149	0.155 \pm 0.062	1.40 \pm 0.047 ^b	0.593 \pm 0.158
DHAP	0.036 \pm 0.005	0.017 \pm 0.004	0.055 \pm 0.001	0.035 \pm 0.005
GAP ($\times 10^3$) (calculated)	1.62 \pm 0.241	0.791 \pm 0.179	2.50 \pm 0.042 ^b	1.58 \pm 0.221
1,3-P ₂ -glycerate ($\times 10^3$) (calculated)	0.869 \pm 0.081	3.32 \pm 0.076 ^b	3.57 \pm 1.10 ^b	2.57 \pm 0.440 ^b
2,3-P ₂ -glycerate	0.010 \pm 0.004	0.008 \pm 0.001	0.007 \pm 0.002	0.010 \pm 0.004
3-P-glycerate	0.071 \pm 0.004	0.063 \pm 0.003	0.064 \pm 0.018	0.042 \pm 0.006 ^b
2-P-glycerate	0.009 \pm 0.002	0.003 \pm 0.003 ^b	<0.002	0.002 \pm 0.001 ^b
P-enolpyruvate	0.013 \pm 0.003	0.008 \pm 0.008	0.011 \pm 0.006	0.002 \pm 0.002 ^b
Pyruvate	0.055 \pm 0.004	0.036 \pm 0.003 ^b	0.085 \pm 0.004 ^b	0.060 \pm 0.009
L-Lactate	0.683 \pm 0.053	0.288 \pm 0.064 ^b	0.737 \pm 0.079	0.778 \pm 0.247
Citrate	0.432 \pm 0.042	1.15 \pm 0.076 ^b	0.883 \pm 0.031 ^b	1.56 \pm 0.210 ^b
Isocitrate	0.018 \pm 0.002	0.065 \pm 0.004 ^b	0.051 \pm 0.002 ^b	0.092 \pm 0.009 ^b
Fru-2,6-P ₂ ($\times 10^3$)	11.3 \pm 1.54	6.45 \pm 1.72	8.39 \pm 2.90	7.80 \pm 0.51 ^b

^a $[\text{Glycogen}]$ was 35.3 \pm 3.17 μmol of glucosyl units/ml of intracellular water at the end of the 15-min stabilization period.

^b $p < 0.05$, Mann-Whitney U test.

the ketones plus insulin group. The activities of the enzymes of glycogen metabolism were analyzed as well as [cAMP], which can affect these enzymes through a cascade of protein kinases (69, 70). No significant change was found in [cAMP] (Table III) or in the percentage of phosphorylase *a*, the phosphorylated form. Total phosphorylase activity is given in Table V. The percentages in the *a* form were 5.6, 4.4, 5.4, and 5.0 in the glucose, ketones, insulin, and ketones plus insulin groups, respectively, suggesting that cytoplasmic free $[Ca^{2+}]$ was not altered by the treatments given. Total glycogen synthase was measured (Table V) and did not vary among the experimental groups. Despite the increases in phosphorylated hexoses, the immediate precursor of glycogen, [UDP-Glc], remained invariant; however, [UTP] decreased with addition of ketones plus insulin, and [UDP] decreased 1.5-fold with all conditions even though glycogen synthesis was increased (Tables I and III).

In contrast to the up to 10-fold increases in metabolites preceding the P-fructokinase (EC 2.7.1.11) step, the concentrations of total Fru-1,6-P₂ were decreased 4-fold by provision of the alternative substrate; ketone bodies increased 2-fold on addition of insulin, but remained unchanged by the combination (Table II, Fig. 1). Because of the large amount of Fru-1,6-P₂ binding to aldolase (EC 4.1.2.13) (49), free [Fru-1,6-P₂] was calculated from the measured [DHAP] and the *K'* of the aldolase and triose-P isomerase reactions (Table IV). The free [Fru-1,6-P₂] was calculated to be 0.68 nmol/ml of intracellular water in hearts perfused with glucose alone and was altered by additions to the perfusate to the same degree as total [Fru-1,6-P₂] (Table II, Fig. 1). The [Fru-2,6-P₂], a positive effector of P-fructokinase (71, 72), was 11.3 nmol/ml of intracellular water in the glucose-perfused hearts and was 6.5 on addition of ketones, thus paralleling the changes in [Fru-1,6-P₂]. In agreement with previous reports, insulin did not increase [Fru-2,6-P₂] in the perfused hearts (73, 74).

[DHAP] was 0.036 μ mol/ml of intracellular water in glucose-perfused hearts and increased 2.7-fold on addition of insulin, but it was unchanged on addition of ketones and the combination. [1,3-P₂-glycerate], calculated from the *K'* of the 3-P-glycerate kinase reaction and the measured levels of [3-P-glycerate] and cytoplasmic $[\Sigma ATP]/[\Sigma ADP]$, was 0.87 μ mol/ml of intracellular water in glucose-perfused hearts, increased 3-fold on addition of ketones or insulin, and increased 2-fold on addition of the combination, reflecting the increase in the $[\Sigma ATP]/[\Sigma ADP]$. Whereas both the GAP dehydrogenase (EC 1.2.1.12) and the 3-P-glycerate kinase reactions have long been considered to be at near-equilibrium *in vivo* (75), the latter reaction was chosen for the calculation of [1,3-P₂-glycerate] because the *V*_{max} forward of 3-P-glycerate kinase is 15,000 μ mol/min/ml of intracellular water, compared with 300 for that of the GAP dehydro-

genase reaction and is 1 or 2 orders of magnitude greater than the other enzymes of glycolysis (Table V).

[3-P-glycerate] was 0.071 μ mol/ml of intracellular water in hearts perfused with glucose alone and was unchanged on the addition of either ketones or insulin but decreased 1.7-fold on addition of ketones plus insulin. [2-P-glycerate] was decreased >3-fold in all groups as compared with glucose (Table II, Fig. 1),

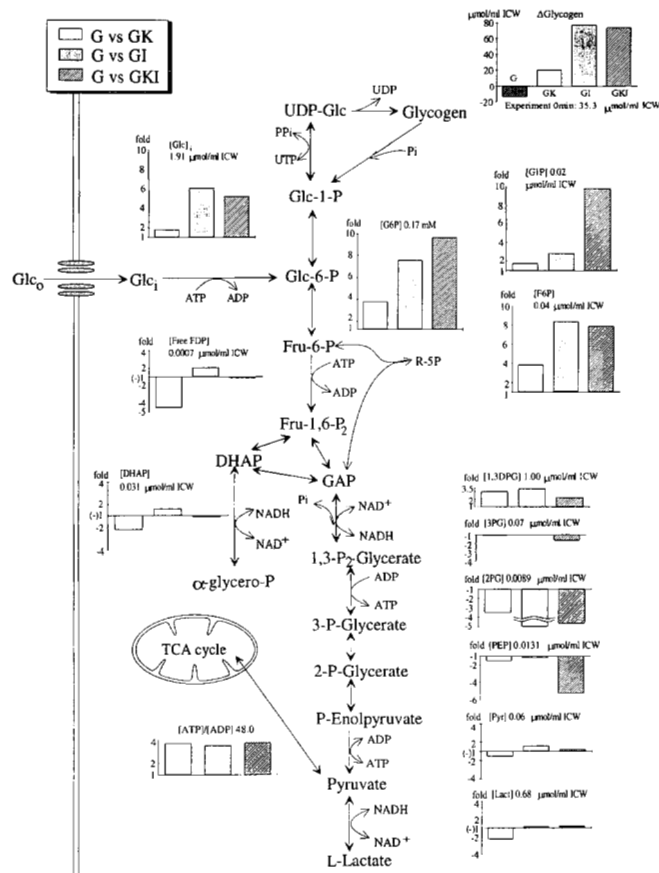


FIG. 1. Metabolite concentrations (μ mol/ml of intracellular water) in working perfused rat heart following the addition of 4 mM sodium D- β -hydroxybutyrate and 1 mM sodium acetoacetate and/or insulin (100 nM). The differences from hearts perfused with glucose alone are shown as proportionate changes as described under "Experimental Procedures," with the concentrations in hearts perfused with glucose alone following the metabolite title; only glycogen is shown as the actual concentration. ICW, intracellular water; G, glucose alone in the perfusate; GK, glucose plus ketone bodies; GI, glucose plus insulin; GKI, glucose plus ketones and insulin; TCA cycle, tricarboxylic acid cycle.

TABLE III
Nucleotides, calculated pH, and free $[Mg^{2+}]$ in perfused working rat hearts

Values are μ mol/ml of intracellular water \pm S.E. for the number of observations given in Table II. The calculations of free $[Mg^{2+}]$ and cytoplasmic $[\Sigma ATP]/[\Sigma ADP]$ are described under "Experimental Procedures." Cytoplasmic pH and $[P_i]$ were from ^{31}P NMR. Significant differences from glucose-perfused hearts are indicated.

	Glucose	Glucose + ketones	Glucose + insulin	Glucose + ketones + insulin
pH	7.06 \pm 0.01	7.05 \pm 0.01	7.04 \pm 0.02	7.02 \pm 0.00 ^a
Free $[Mg^{2+}]$	1.23 \pm 0.03	0.744 \pm 0.011 ^a	0.730 \pm 0.029 ^a	0.666 \pm 0.082 ^a
cAMP ($\times 10^3$)	0.864 \pm 0.031	0.740 \pm 0.044	0.629 \pm 0.104	0.856 \pm 0.200
UTP	0.194 \pm 0.010	0.161 \pm 0.021	0.179 \pm 0.006	0.159 \pm 0.005 ^a
UDP	0.034 \pm 0.002	0.021 \pm 0.002 ^a	0.025 \pm 0.001 ^a	0.022 \pm 0.001 ^a
UDP-Glc	0.099 \pm 0.006	0.109 \pm 0.015	0.096 \pm 0.003	0.094 \pm 0.001
Phosphocreatine	6.84 \pm 0.376	14.7 \pm 1.30 ^a	17.1 \pm 0.530 ^a	16.4 \pm 0.567 ^a
Creatine	23.9 \pm 1.51	12.1 \pm 1.49 ^a	13.7 \pm 1.14 ^a	12.5 \pm 0.488 ^a
Cytoplasmic free $[P_i]$	6.94 \pm 1.37	7.81 \pm 1.00	4.88 \pm 0.66	6.42 \pm 2.22
Cytoplasmic $[\Sigma ATP]/[\Sigma ADP]$	45.4 \pm 2.55	168 \pm 8.93 ^a	166 \pm 9.50 ^a	179 \pm 8.93 ^a

^a $p < 0.05$, Mann-Whitney U test.

TABLE IV

Equilibrium constants of the reactions of glucose and glycogen metabolism compared with the ratio of [products] to [reactants] in perfused working rat hearts

The equilibrium constants (K') have been corrected (62) where necessary for differences in tissue pH and free $[Mg^{2+}]$ (Table II). The values of [products]/[reactants] (Γ) are taken from Tables II and III. The reactions of UDP-Glc pyrophosphorylase, aldolase, triose-P isomerase, GAP dehydrogenase, 3-P-glycerate kinase, and pyruvate kinase are assumed to be at near-equilibrium, and Γ/K' is given as 1. The values for K' given at various pH and free $[Mg^{2+}]$ are those for the sum of the species present. The reactions written are those of the most ionized species.

Reaction		Glucose	Glucose + ketones	Glucose + insulin	Glucose + ketones + insulin
Glycogen synthase (EC 2.4.1.11)	K'^a	37.7	29.8	29.5	28.6
UDP-Glc $^{2-}$ + Glc $_n$ \rightarrow UDP $^{3-}$ + Glc $_{n+1}$ + H $^+$	Γ	0.343	0.193	0.261	29.14
	Γ/K'	9.08×10^{-3}	6.47×10^{-3}	8.85×10^{-3}	8.23×10^{-3}
Phosphorylase (EC 2.4.1.1)	K'^b	0.719	0.723	0.727	0.716
Glc $_n$ + P $_i^{2-}$ \rightarrow Glc $_{n-1}$ + Glc-1-P $^{2-}$	Γ	2.90×10^{-3}	4.47×10^{-3}	1.16×10^{-2}	3.08×10^{-2}
	Γ/K'	4.03×10^{-3}	6.19×10^{-3}	1.60×10^{-2}	4.30×10^{-2}
UDP-Glc pyrophosphorylase (EC 2.7.7.9)	K'^c	4.36	3.47	3.34	3.46
Glc-1-P $^{2-}$ + UTP $^{4-}$ + H $^+$ \rightarrow UDP-Glc $^{2-}$ + HPP $_i^{3-}$	Γ	4.36	3.47	3.34	3.46
	Γ/K'	1	1	1	1
Glucose transporter	K'	1	1	1	1
Glc $_o$ \rightarrow Glc $_i$	Γ	0.191	0.340	>1	0.994
	Γ/K'	0.191	0.340	>1	0.994
Hexokinase (EC 2.7.1.1)	K'^d	2.09×10^3	2.42×10^3	2.49×10^3	2.43×10^3
Glc + ATP $^{4-}$ \rightarrow Glc-6-P $^{2-}$ + ADP $^{3-}$ + H $^+$	Γ	1.94×10^{-3}	1.08×10^{-3}	6.64×10^{-4}	9.14×10^{-4}
	Γ/K'	9.29×10^{-7}	4.45×10^{-7}	2.67×10^{-7}	3.76×10^{-7}
P-glucomutase (EC 5.4.2.2)	K'^e	16.2	0.0617 o	0.0617 o	0.0617 o
Glc-1-P $^{2-}$ \rightarrow Glc-6-P $^{2-}$ (glucose group)	Γ	8.40	0.057	0.045	0.122
Glc-6-P $^{2-}$ \rightarrow Glc-1-P $^{2-}$ (other groups) o	Γ/K'	0.518	0.924	0.725	>1
P-glucoisomerase (EC 5.3.1.9)	K'^f	0.30	0.30	0.30	0.30
Glc-6-P $^{2-}$ \rightarrow Fru-6-P $^{2-}$	Γ	0.240	0.253	0.270	0.198
	Γ/K'	0.800	0.842	0.898	0.659
P-fructokinase (EC 2.7.1.11)	K'^g	1.32×10^3	1.53×10^3	1.58×10^3	1.54×10^3
Fru-6-P $^{2-}$ + ATP $^{4-}$ \rightarrow Fru-1,6-P $_2^{4-}$ + ADP $^{3-}$ + H $^+$	Γ	3.69×10^{-4}	6.00×10^{-6}	2.47×10^{-5}	1.03×10^{-5}
	Γ/K'	2.80×10^{-7}	3.92×10^{-9}	1.56×10^{-8}	6.70×10^{-9}
Aldolase (EC 4.1.2.13)	$K' (M^{-1})^h$	9.87×10^{-5}	9.82×10^{-5}	9.80×10^{-5}	9.83×10^{-5}
Fru-1,6-P $_2^{4-}$ \rightarrow DHAP $^{2-}$ + GAP $^{2-}$	Γ	9.87×10^{-5}	9.82×10^{-5}	9.80×10^{-5}	9.83×10^{-5}
	Γ/K'	1	1	1	1
Triose-P isomerase (EC 5.3.1.1)	K'^i	0.046	0.046	0.046	0.046
DHAP $^{2-}$ \rightarrow GAP $^{2-}$	Γ	0.046	0.046	0.046	0.046
	Γ/K'	1	1	1	1
GAP dehydrogenase (EC 1.2.1.12)	K'^j	6.04×10^{-1}	5.82×10^{-1}	6.00×10^{-1}	5.50×10^{-1}
GAP $^{2-}$ + P $_i^{2-}$ + NAD $^+$ \rightarrow 1,3-P $_2$ -glycerate $^{4-}$ + NADH + H $^+$	Γ	6.04×10^{-1}	5.82×10^{-1}	6.00×10^{-1}	5.50×10^{-1}
	Γ/K'	1	1	1	1
3-P-glycerate kinase (EC 2.7.2.3)	K'^k	3767	3094	3075	2942
1,3-P $_2$ -glycerate $^{4-}$ + ADP $^{3-}$ \rightarrow 3-P-glycerate $^{3-}$ + ATP $^{4-}$	Γ	3767	3094	3075	2942
	Γ/K'	1	1	1	1
3-P-glycerate mutase (EC 5.4.2.1)	K'^l	0.11	0.11	0.11	0.11
3-P-glycerate $^{3-}$ \rightarrow 2-P-glycerate $^{3-}$	Γ	0.125	0.071	0.047	0.076
	Γ/K'	>1	0.648	0.424	0.689
Enolase (EC 4.2.1.11)	K'	4.0	4.0	4.0	4.0
2-P-glycerate $^{3-}$ \rightarrow P-enolpyruvate $^{3-}$	Γ	1.47	2.30	>4.0	1.39
	Γ/K'	0.368	0.574	>1	0.348
Pyruvate kinase (EC 2.7.1.40)	K'^m	1.20×10^4	1.10×10^4	1.07×10^4	1.09×10^4
P-enolpyruvate $^{3-}$ + ADP $^{3-}$ + H $^+$ \rightarrow Pyruvate $^-$ + ATP $^{4-}$	Γ	1.91×10^2	5.82×10^2	1.18×10^3	2.44×10^3
	Γ/K'	1.58×10^{-2}	5.32×10^{-2}	1.11×10^{-1}	2.23×10^{-1}
Lactate dehydrogenase (EC 1.1.1.28)	K'^n	7.85×10^4	8.22×10^4	8.03×10^4	8.60×10^4
Pyruvate $^-$ + NADH + H $^+$ \rightarrow L-Lactate $^-$ + NAD $^+$	Γ	7.85×10^4	8.22×10^4	8.03×10^4	8.60×10^4
	Γ/K'	1	1	1	1

a R. N. Goldberg, personal communication. Calculated from ΔG° values for the hydrolysis of sucrose (41) and maltose (42) and synthesis of sucrose (43), b (44), c (45), d (46), e (47), f (48), g (46), h (49), i (50), j (51), k (51), l (52), m (53), n (54).

o $p < 0.05$, Mann-Whitney U test.

and after perfusion with insulin it was not detectable by our methods. There was, however, no change in [2,3-P $_2$ -glycerate], indicating that the decrease in [2-P-glycerate] did not result

from lack of the cofactor for 3-P-glycerate mutase. [P-enolpyruvate] was significantly decreased in the presence of ketones with insulin but was unchanged in the other experimental

TABLE V
Kinetic parameters of the enzymes of glucose and glycogen metabolism

The kinetics of the glycolytic enzymes were measured in 10 mM P_i , 20 mM imidazole buffer, pH 7.2, 150 mM KCl, and 5 mM total magnesium at 38 °C. Activity is expressed as $\mu\text{mol}/\text{min}/\text{ml}$ of intracellular water \pm S.E., and K_{mS} values are expressed as mM. The number of observations is 3. V_{maxF} and K_{mS} denote the velocity and K_m in the direction of L-lactate formation (forward); V_{maxR} and K_{mP} denote the same parameters in the opposite direction (reverse).

Enzyme	V_{maxF}	K_{mS}	V_{maxR}	K_{mP}	K_m nucleotide or P_i
Glycogen synthase					
I form	8.81 \pm 1.65	0.08 ^a			
D form	8.81 \pm 1.65	1.42 ^a			
Phosphorylase ^b	46.9 \pm 2.56	0.1 ^c	3350	5 ^c	
P-glucomutase	116 \pm 16.6	0.045	67.2 \pm 3.15	0.67	
Glc-1-P \rightarrow Glc-6-P					
Glucose transport ^d					
Glucose	4	2			
3-O-Methylglucose					
Without insulin	0.14–1	7–10	1–0.01	7	
With insulin	13.2	6	6.6	3	
Hexokinase	33 \pm 1.35	0.072	0.00637 ^e	0.042 ^e	0.236 (ATP)
Glucose-6-phosphatase	ND ^f				
Glc-6-P dehydrogenase	5.70				
P-glucoisomerase	604 \pm 47.8	0.425	576 \pm 12.5	0.175	
P-fructokinase	79.7 \pm 8.26	0.224			0.127
Aldolase	59.5 \pm 2.50	0.038			
Triose-P isomerase	356 \pm 32.5	1.53			
GAP dehydrogenase	321 \pm 28.7	0.042			0.058 (NAD ⁺) ^g 1.42 (P_i) 0.008 (ADP) 0.565 (ATP)
3-P-glycerate kinase	15,060 \pm 175	0.021	959 \pm 169	0.51	
3-P-glycerate mutase	674 \pm 77.8	0.145	2880 \pm 101	0.139	
Enolase	111 \pm 6.22	0.045	120 \pm 7.40	0.089	
Pyruvate kinase	566 \pm 18.6	0.11	0.63 ^h	10 ^h	0.268 (ADP)
Lactate dehydrogenase	1436 \pm 36.6	0.125			0.001 (NADH) ⁱ

^a K_{mS} for the I and D forms in the presence of Glc-6-P (55).

^b V_{maxF} was calculated by Haldane's relationship.

^c Ref. 56.

^d Ref. 4, $\mu\text{mol}/\text{g}$ wet weight.

^e Calculated from Ref. 57.

^f Not detected.

^g K_m for NAD⁺ was increased by increasing [P_i], and K_m for P_i was increased by increasing [GAP]. The value for NAD⁺ reported here is in the presence of 5 mM P_i , and that for P_i is in the presence of 0.036 mM GAP.

^h Ref. 53.

ⁱ K_m for NADH was increased in the presence of increased [pyruvate]. The value reported here was determined in the presence of 0.022 mM pyruvate.

groups despite the decrease in the precursor, [2-P-glycerate]. [Pyruvate] was 0.055 $\mu\text{mol}/\text{ml}$ of intracellular water in hearts perfused with glucose alone, decreased 1.5-fold on addition of ketones, increased 1.5-fold on addition of insulin, and was unchanged on addition of ketones plus insulin. [L-Lactate] was 0.68 $\mu\text{mol}/\text{ml}$ of intracellular water in hearts perfused with glucose alone and decreased 2.3-fold on the addition of ketones but was unchanged on the addition of insulin or insulin plus ketones. The L-lactate efflux increased 1.7-, 13.3-, and 2.2-fold in the presence of ketones, insulin, or the combination, respectively.

The values of the equilibrium constants (K') of the reactions catalyzed by the enzymes of glucose metabolism, corrected for changes in pH and free [Mg^{2+}] when appropriate, were compared with the values of the [products]/[reactants] of the measured concentrations in heart tissue (Γ) (Table IV). The Γ/K' for the glucose transport reaction was 0.19 during perfusion with glucose alone, 0.34 after addition of ketones, and about 1 on addition of insulin and the combination, showing that insulin equilibrated [Glc_o] and [Glc_i]. The reactions catalyzed by hexokinase and P-fructokinase had Γ/K' ranging from 10^{-7} to 10^{-9} , confirming previous reports in other tissues that these steps were far from equilibrium (45, 76). For the reactions of glycogen synthase and phosphorylase, the Γ/K' ranged between 10^{-2} and 10^{-3} . The Γ/K' of the reaction catalyzed by P-glucoisomerase ranged from 0.90 to 0.66 despite the 10-fold increase in [Glc-6-P], showing that this step is at near-equilibrium under all conditions tested here.

Because the binding of GAP to aldolase distorts the tissue ratios, the Γ/K' values for the reactions catalyzed by aldolase and triose-P isomerase were assumed to be at near-equilibrium (49) and, therefore, were assigned a value of 1. [GAP] was calculated from the measured value of [DHAP] and the K' of the triose-P isomerase reaction. For similar reasons and because of the instability of 1,3- P_2 -glycerate, the tissue levels of this metabolite were not measured but were calculated from the components of the 3-P-glycerate kinase reaction. The values of Γ/K' for the GAP dehydrogenase and the 3-P-glycerate kinase reactions were assigned a value of 1 (51, 75). Γ/K' for the components of the 3-P-glycerate mutase reaction was >1 during perfusion with glucose alone and decreased to 0.65 on addition of ketones or 0.69 with ketones plus insulin, but it decreased to 0.42 on perfusion with insulin alone. Γ/K' for the enolase reaction was 0.37 on perfusion with glucose alone and 0.35 in the presence of ketones plus insulin, but it increased to 0.58 on addition of ketones and to >1 on perfusion with insulin. The apparent changes in the flux control coefficient at the enolase and P-glycerate mutase steps were an unexpected outcome of this type of analysis. The changes did not correlate with changes in the measured amounts of the cofactor of the mutase, 2,3- P_2 -glycerate (Table II). In contrast to the findings with the substrates of the hexokinase and P-fructokinase reactions where Γ/K' was $<10^{-6}$ or the 3-P-glycerate kinase reaction where Γ/K' was 1, the Γ/K' values for the substrates of the pyruvate kinase reaction were a factor of <100 from equilibrium. Γ/K' for the pyruvate kinase reaction was 0.016 during perfusion with glucose alone and in-

TABLE VI
Flux control coefficients determined by bottom-up analysis

Standard errors and coefficients of variation were calculated using MetaCom (68). Errors of 10% were arbitrarily assigned to the elasticities and fluxes used in the calculation of flux control coefficients in order to calculate the sensitivity and error analysis. Values are given \pm S.E.; the coefficient of variation (S.D. mean \times 100) in percent is given in parentheses.

	Glucose	Glucose + ketones	Glucose + insulin	Glucose + ketones + insulin
1. Branched pathway from glucose transport to glycogen metabolism and P-glucoisomerase ^a				
ϵ_{Glc}^{Glut4}	-0.237	-0.516	-100	-100
ϵ_{Glc}^{HK}	0.159	0.248	0.164	0.224
ϵ_{G6P}^{HK}	-0.128	-0.232	-0.159	-0.218
ϵ_{G6P}^{PGM}	-1.22	12.9	3.18	100
ϵ_{G1P}^{PGM}	1.81	-12.5	-2.94	-100
ϵ_{G6P}^{PGI}	4.75	5.91	9.39	2.36
$\epsilon_{G1P}^{UDPGlase}$	NA ^b	100	100	100
$\epsilon_{UDPGlc}^{UDPGlase}$	NA ^b	-100	-100	-100
$\epsilon_{UDPGlc}^{GlycS}$	NA	0.929	0.455	0.461
ϵ_{G1P}^{Plase}	-0.011	NA	NA	NA
C_{Glut4}^J	0.396 \pm 0.34 (9.2)	0.314 \pm 0.030 (9.6)	0.002 \pm 0.0002 (10)	0.002 \pm 0.0003 (15)
C_{HK}^J	0.590 \pm 0.033 (5.6)	0.653 \pm 0.029 (4.4)	0.972 \pm 0.003 (0.31)	0.862 \pm 0.017 (1.9)
C_{PGM}^J	<0.001	0.001 \pm 0.0002 (20)	0.001 \pm 0.0002 (20)	<0.001
C_{PGI}^J	0.016 \pm 0.002 (13)	0.024 \pm 0.003 (13)	0.016 \pm 0.003 (19)	0.066 \pm 0.008 (12)
$C_{UDPGlase}^J$	NA	<0.001	<0.001	<0.001
C_{GlycS}^J	NA	0.009 \pm 0.002 (22)	0.009 \pm 0.002 (22)	0.069 \pm 0.011 (16)
C_{Plase}^J	-0.001 \pm 0.0001 (10)	NA	NA	NA
2. Linear pathway from 3-P-glycerate kinase to pyruvate kinase ^c				
ϵ_{3PG}^{PGK}	-100	-100	-100	-100
ϵ_{3PG}^{PGlyM}	100	2.50	1.39	3.00
ϵ_{2PG}^{PGlyM}	-100	-1.82	-0.702	-2.24
ϵ_{2PG}^{Eno}	1.43	2.27	100	1.47
ϵ_{PEP}^{Eno}	-0.687	-1.45	-100	-0.577
ϵ_{PEP}^{PK}	0.859	0.929	0.981	1.23
C_{PGK}^J	0.008 \pm 0.002 (25)	0.008 \pm 0.001 (13)	0.008 \pm 0.001 (13)	0.009 \pm 0.002 (22)
C_{PGlyM}^J	0.008 \pm 0.001 (13)	0.326 \pm 0.036 (11)	0.575 \pm 0.048 (8.3)	0.306 \pm 0.31 (11)
C_{Eno}^J	0.547 \pm 0.034 (6.2)	0.260 \pm 0.019 (7.3)	0.004 \pm 0.0004 (10)	0.466 \pm 0.025 (5.4)
C_{PK}^J	0.438 \pm 0.035 (8.0)	0.406 \pm 0.039 (9.6)	0.412 \pm 0.048 (12)	0.219 \pm 0.029 (11)

^a Scheme 1.

^b NA, not applicable.

^c Scheme 2.

creased to 0.053 on addition of ketones, 0.11 on addition of insulin, and 0.22 on addition of the combination. There was no correlation between the shifts for the pyruvate kinase reaction and the [Fru-1,6-P₂] or [Fru-2,6-P₂].

Using bottom-up analysis of the upper portion of glucose metabolism (Scheme 1), from extracellular glucose to Fru-6-P and glycogen (Table VI, part 1), the flux control coefficient of glucose transporter (C_{Glut4}^J) was 0.40, of hexokinase (C_{HK}^J) was 0.59, of P-glucoisomerase (C_{PGI}^J) was 0.02, and of phosphorylase (C_{Plase}^J) was -0.001 during perfusion with glucose alone. The activity of glucose-6-phosphatase was not considered since we were unable to detect it *in vitro*, although this activity has been inferred from NMR data.³ The addition of ketones slightly increased control at the hexokinase and P-glucoisomerase steps; some control appeared at the glycogen synthase step (C_{GlycS}^J). Insulin essentially abolished control at the glucose transporter; $C_{Glut4}^J = 0.002$, $C_{HK}^J = 0.97$, $C_{PGI}^J = 0.02$, and $C_{GlycS}^J = 0.01$. In the presence of insulin and ketones, control was shared by hexokinase, P-glucoisomerase, and glycogen synthase; $C_{HK}^J = 0.86$, $C_{PGI}^J = 0.07$, and $C_{GlycS}^J = 0.07$.

In the terminal glycolytic portion of bottom-up analysis (Scheme 2), from 1,3-P₂-glycerate to pyruvate (Table VI, part 2) in the presence of glucose only, the flux control coefficient of

enolase (C_{Eno}^J) was 0.55 and of pyruvate kinase (C_{PK}^J) was 0.44, whereas the flux coefficients of 3-P-glycerate kinase (C_{PGK}^J) and 3-P-glycerate mutase (C_{PGlyM}^J) were <0.01. After addition of ketones, insulin, or both, C_{PGlyM}^J was 0.33, 0.58, and 0.31, respectively. C_{Eno}^J was decreased to 0.26 after addition of ketones and to 0.47 in the presence of ketones plus insulin, but it was reduced to nearly 0 in the presence of insulin and absence of ketones. C_{PK}^J was not changed in the presence of ketones or insulin, but it was decreased to 0.22 in the presence of the combination.

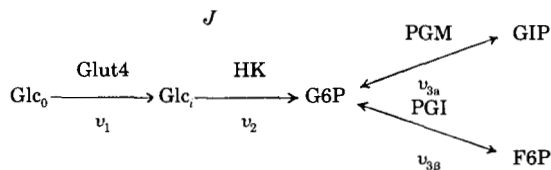
Using top-down analysis with Glc-6-P as the intermediate between blocks (Scheme 3), C_1^J comprising the block of glucose transport and phosphorylation step was 0.58, C_2^J of the block comprising glycogen synthesis was 0.17, and C_3^J of the block comprising glycolysis was 0.26. This type of analysis confirmed that glucose entry and phosphorylation dominated the control of glucose metabolism, with glycolysis exerting about a quarter and glycogen synthesis 17% of the control of the total rate (Table VII, part 1). Top-down analysis was performed with [Glc_i] as the intermediate between blocks composed of (Scheme 4) C_1^J , the glucose transporter, and C_2^J , all of the other reactions of glucose utilization. In the presence of ketones, the control distribution was similarly shared between the two blocks; $C_1^J = 0.55$ and $C_2^J = 0.45$ (no significant difference). This contrasts with the states involving addition of insulin where C_1^J de-

³ K. Clarke, personal communication.

creased to nearly zero, while the control exerted by the combined pathways of glucose utilization increased to 0.99 (Table VII, part 2). Although these top-down results are approximate, they offer corroboration (via an independent method of analyzing the results) of the conclusion from the bottom-up analysis that in the absence of insulin the transporter shares some of the control but that in the presence of insulin the control shifts to glucose utilization.

DISCUSSION

In a metabolic pathway in the steady state,



the flux (J) through the pathway is equal to the net rate (v) for any single enzyme step, all of which are equal. Since $v_1 = v_2 = v_{3a} + v_{3b} = J$, it is true, but misleading, to say that the flux through the pathway is equal to the "slowest" or "pacemaker" enzyme since the flux through all of the steps is equal in the steady state. By assigning flux control coefficients to each step or to blocks of steps and by setting $\sum C^J = 1$ (the summation theorem, Equation 9), metabolic control analysis attempts to define formally the proportion of a change in the flux that is caused by changes either in the reactants or in the kinetic properties of each particular step in an arbitrarily defined pathway. This analysis shows that control of metabolic flux can be distributed between several enzymatic steps and that the site and degree of control may vary. Thus control of the flux of glucose utilization varies with the nutrient presented or the receptor stimulated. This has implications for both genetic and pharmacological therapy in that alteration in the degree of flux control at one step will result in the development of flux control at other steps. It is therefore necessary to understand the metabolic system as a whole and not simply focus narrowly on one or another enzyme step within the pathway.

Flux control coefficients may be derived from the elasticity of each enzyme step using the connectivity theorem (Equation 10, $\sum C^J_{E_i} \epsilon^{E_i}_x = 0$). Elasticities of small magnitude are critical; large elasticities have relatively little influence on the flux control coefficient. If two adjacent enzymes have a large and small elasticity, respectively, for a common intermediate, the enzyme with the small elasticity will have the larger flux control coefficient. A negative value for elasticity means an inhibitory effect (elasticities embody the kinetic effects). For example, with $[Glc_i]$ as the common intermediate, the glucose transporter and hexokinase are adjacent enzymes. Equation 10 can be described as $C^{J_{Glut4}}_{Glc_i} \epsilon^{Glut4}_{Glc_i} + C^{J_{HK}}_{Glc_i} \epsilon^{HK}_{Glc_i} = 0$. The value of $\epsilon^{Glut4}_{Glc_i}$ was -0.24 , and $\epsilon^{HK}_{Glc_i}$ was 0.16 in the glucose group; $C^{J_{Glut4}}$ was 0.40 , and $C^{J_{HK}}$ was 0.59 .

As long as the flux control coefficient can be obtained from the elasticities, the change in flux is a result of changes in either the inherent kinetic properties of the enzyme or in the ratio of [products] to [reactants] for that enzyme. The explanation for this relationship may be seen from the derivation of elasticities (Equation 8), which are a function of K' for the reaction, the ratio of [products] to [reactants] actually achieved under the condition studied (here called Γ), and K_m and V_{max} in the forward and backward direction for each enzyme. In the case of the enzymes of glucose utilization in the perfused heart, the elasticities for each step fall into three classes depending upon how close they come to catalyzing equilibrium between their products and reactants under the conditions studied.

When Γ/K' of an enzyme-catalyzed reaction is >0.5 (close to equilibrium), the elasticity depends primarily on the value of Γ/K' , and as Γ/K' increases, the value of ϵ increases in a manner resembling an exponential curve. In perfused hearts, this situation pertains to the P-glucosomerase and P-glucomutase reactions (Table IV). Analytically, it is difficult to distinguish between 0.5 and 1 of Γ/K' ; however, in this range the elasticity will change by orders of magnitude and will, in turn, affect the calculation of the flux control coefficients. In some instances, this relationship assigns flux control coefficients that appear to vary disproportionately with the observed changes in $[S]$. For example, in the cases of enolase and P-glycerate mutase, small changes in $[2\text{-P-glycerate}]$ and $[P\text{-enolpyruvate}]$ resulted in the shift of control from one enzyme to the other. The low concentrations lend a degree of uncertainty to the measurement of these metabolites, which in some conditions were below the range of accurate detection.

When Γ/K' is >0.01 but <0.5 , elasticity is a function both of the ratio of [products] to [reactants] and of the kinetic constants for the enzyme. An example of such a reaction is the insulin-sensitive glucose transporter, Glut4 (7). During perfusion with glucose alone, Γ/K' was 0.19 , and thus Glut4 would be sensitive not only to changes in the ratio of [products] to [reactants] but also to changes in the kinetic constants of the enzyme. Both mechanisms were demonstrated here. By the first mechanism, addition of ketones decreased the demand for glucose and resulted in an increase in $[Glc_i]$ from 1.9 to $3.5 \mu\text{mol/ml}$ of intracellular water (Table II). The elevation in [product] increased Γ/K' from 0.19 to 0.34 , altering $\epsilon^{Glut4}_{Glc_i}$ from -0.24 to -0.52 (Table VI). Second, addition of insulin changed the kinetic constants of the glucose transporter by increasing V_{max} 10-fold (Table V), which increased $[Glc_i]$ to near $10 \mu\text{mol/ml}$ of intracellular water (Table II), making Γ/K' near 1 ; and thus $\epsilon^{Glut4}_{Glc_i}$ was increased to negative infinity (-100 was arbitrarily assigned) with a consequent decrease in $C^{J_{Glut4}}$ to nearly zero. The very low flux control coefficient of the glucose transporter in the presence of insulin means that under conditions of saturating doses of insulin, glucose transport no longer plays a significant role in the control of glucose utilization. In the case of the hexokinase reaction, product inhibition by Glc-6-P significantly decreases the flux control coefficient of this step below what it might be were such inhibition not present. The significance of this effect has been pointed out by other workers (77).

In those enzymes that catalyze reactions that are far from equilibrium so that Γ/K' is <0.01 , such as hexokinase, P-fructokinase, and (in most cases) glycogen synthase and phosphorylase, the elasticity is totally insensitive to changes in Γ/K' and responds only to changes in kinetic constants.

The flux control coefficient is also affected by the ratio of the fluxes in the branches, which is equivalent to the ratio of the flux control coefficients (the branch point theorem, Equation 11). Despite the small elasticities of glycogen synthase and phosphorylase, $C^{J_{Glycs}}$ in the presence of ketones, insulin, and ketones plus insulin and $C^{J_{Plase}}$ in the presence of glucose were small; this is in part a consequence of the flux ratios. $C^{J_{Glycs}}$ and $C^{J_{Plase}}$ were also affected by the neighboring UDP-Glc pyrophosphorylase and P-glucomutase reactions with large elasticities. Finally, the flux control coefficients were obtained by using matrix algebra (Equations 12, 15, 17, 20, 22, and 24); the proportion of control will be affected by each elasticity, the ratio of the fluxes, and the other flux control coefficients in the system.

The conversion from glycogen phosphorylase to glycogen synthase was achieved in two ways. First, the requirement for glucose was decreased by providing ketone bodies as an alternative substrate for oxidative phosphorylation, permitting the accumulation of glucose and Glc-6-P. Second, in the presence of

TABLE VII
 Flux control coefficients determined by top-down analysis

Standard errors and coefficients of variation were obtained and are presented as described in Table VI.

1. Glc-6-P as intermediate ^a						
Block	Control	Addition	ε	C		
1. Glucose transport and phosphorylation	Glucose	Ketones	$\varepsilon_{\text{G6P}}^1$	-0.51 ± 0.26	C_1^J	0.58 ± 0.17 (29)
2. Glycogen synthesis	Ketones	Insulin	$\varepsilon_{\text{G6P}}^2$	1.34 ± 0.47	C_2^J	0.17 ± 0.07 (42)
3. Glycolysis	Ketones	Insulin	$\varepsilon_{\text{G6P}}^3$	0.264 ± 0.48	C_3^J	0.26 ± 0.11 (42)
2. Glc _i as intermediate ^b						
Block 2		Control	Change	Value		
$\varepsilon_{\text{Glc}_i}^2$	Glycogen synthesis and glycolysis	Glucose	Insulin	0.18 ± 0.10		
$\varepsilon_{\text{Glc}_i}^2$		Ketones	Insulin	0.63 ± 0.35		
	Glucose	Glucose + ketones	Glucose + insulin	Glucose + ketones + insulin		
$\varepsilon_{\text{Glc}_i}^1$	-0.237	-0.516	-100	-100		
$\varepsilon_{\text{Glc}_i}^2$	0.18	0.63	0.18	0.63		
C_1^J	0.43 ± 0.14 (33)	0.55 ± 0.14 (25)	0.002 ± 0.001 (50)	0.006 ± 0.004 (67)		
C_2^J	0.57 ± 0.14 (25)	0.45 ± 0.14 (31)	0.998 ± 0.001 (0.10)	0.994 ± 0.004 (0.40)		

^a Scheme 3.

^b Scheme 4. $\varepsilon_{\text{Glc}_i}^{\text{Glut4}}$ of the glucose transporter as given in Table VI was used for calculation.

insulin, $[\text{Glc}_i]$ was equal to $[\text{Glc}_o]$ as a result of the mobilization of Glut4, and $[\text{Glc-6-P}]$ was elevated up to 10-fold. In both instances, the elevated $[\text{Glc-6-P}]$ can increase the affinity of glycogen synthase for UDP-Glc as much as 6-fold, regardless of the phosphorylation state of the synthase (55).

From the point of view of the kinetics of the enzymes of a pathway and the thermodynamics of the reactions catalyzed, there is nothing fundamentally new in the presentation of results using metabolic control analysis. However, the use of the equations developed does provide a rigor that can help in avoiding imprecise conclusions. The idea that glucose transport is rate-limiting for the reactions of glucose utilization (4, 5, 18) would not appear to be true in working perfused rat heart even in the absence of insulin (Table VI). Rather, the glucose transporter would appear to share with hexokinase the major control of glucose utilization. There remain, however, unexplained observations about hexokinase. The accumulation of Glc-6-P would lead us to predict that hexokinase would be strongly inhibited (78), but the glucose flux was unrelated to $[\text{Glc-6-P}]$; $^3\text{H}_2\text{O}$ released was reduced in the presence of ketones when $[\text{Glc-6-P}]$ was increased 3.6 times but was elevated in the presence of insulin and unchanged in the presence of ketones plus insulin, when $[\text{Glc-6-P}]$ was elevated 8- and 10-fold, respectively (Table I).

In bottom-up analysis, the flux control coefficients indicate the distribution within that selected pathway only; they would all be scaled down if the whole of glucose metabolism was considered. Viewed from the perspective of the processes of glucose utilization, and using top-down analysis, the proportion of control of the block of glucose transporter and phosphorylation, glycogen metabolism, and glycolysis was determined with $[\text{Glc-6-P}]$ assigned as the intermediate metabolite. The flux control coefficient of glucose transport and phosphorylation was 0.58, that of glycogen synthesis was 0.17, and all of glycolysis was 0.26, which is an approximate average over the states considered (Table VII, part 1). It is clear from this study that, considering glucose metabolism as a whole, the activity of P-fructokinase is not the pacemaker, since only 0.26 of the control of glucose utilization is found in all of the steps below P-glucosomerase. That is not to say that P-fructokinase does not have an elegant system of controls that involve an increasing number of previously unknown effectors formed by enzymes

undergoing covalent modification (71, 72, 79). However, the flux through the branches of Fru-6-P and GAP into the nonoxidative portion of the hexose monophosphate pathway (80) and purine synthesis and salvage (81) and the flux through the branch of DHAP to α -glycero-P and the α -glycero-P shuttle (82) (Fig. 1) were not measured. The absence of precise flux measurements through P-fructokinase and the multiple branch points above and below the P-fructokinase reaction precludes the possibility of performing bottom-up analysis at the P-fructokinase step in this study.

In addition to preventing misstatement, the application of this formal approach to an entire pathway provides new insights that may further our understanding of control. An example is the finding that Γ/K' values for phosphorylase, pyruvate kinase, and P-glycerate mutase range from 0.01 to 0.5 and thus have characteristics more in common with the glucose transporter than with enzymes of the type such as hexokinase, P-fructokinase, and glycogen synthase on the one hand (where Γ/K' is <0.01) or with P-glucosomerase on the other (where Γ/K' is >0.5). Enzymes that have intermediate values of Γ/K' might be expected to change the degree to which they may affect flux through the lower portion of glycolysis in response to changes in substrate and product concentrations and to changes in their fundamental kinetic parameters.

Acknowledgments—We thank Dr. R. N. Goldberg for the calculation of K' for glycogen synthase and Dr. Kieran Clarke and C. Keon for the measurements of pH and cytoplasmic P_i in the perfused hearts by NMR.

REFERENCES

1. Lundsgaard, E. (1939) *Upsala Läk. Fören. Förh.* **45**, 143–152
2. Levine, R., Goldstein, M., Klein, S., and Huddleston, B. (1949) *J. Biol. Chem.* **179**, 985–986
3. Morgan, H. E., Regen, D. M., and Park, C. R. (1964) *J. Biol. Chem.* **239**, 369–374
4. Cheung, J. Y., Conover, C., Regen, D. M., Whitfield, C. F., and Morgan, H. E. (1978) *Am. J. Physiol.* **234**, E70–E78
5. Neely, J. R., Liebermeister, H., and Morgan, H. E. (1967) *Am. J. Physiol.* **212**, 815–822
6. Gliemann, J., and Rees, W. D. (1983) *Curr. Top. Membr. Transp.* **18**, 339–379
7. Gould, G. W., and Holman, G. D. (1993) *Biochem. J.* **295**, 329–341
8. Kruckeberg, A. L., Neuhaus, H. E., Feil, R., Gottlieb, L. D., and Stitt, M. (1989) *Biochem. J.* **261**, 457–467
9. Kacser, H., and Burns, J. A. (1973) *Symp. Soc. Exp. Biol.* **27**, 65–104
10. Burns, J. A., Cornish-Bowden, A., Groen, A. K., Heinrich, R., Kacser, H., Porteus, J. W., Rapoport, S. M., Rapoport, T. A., Stucki, J. W., Tager, J. M., Wanders, R. J. A., and Westerhoff, H. V. (1985) *Trends Biochem. Sci.* **10**, 16
11. Fell, D. A., and Sauro, H. M. (1985) *Eur. J. Biochem.* **148**, 555–561

12. Haldane, J. B. S. (1930) in *Enzymes* (Plimmer, R. H. A., and Hopkins, F. G., eds) pp. 74–92, Longmans, Green and Co., London
13. Brown, G. C., Hafner, R. P., and Brand, M. D. (1990) *Eur. J. Biochem.* **188**, 321–325
14. Quant, P. A. (1993) *Trends Biochem. Sci.* **18**, 26–30
15. Groen, A. K., van Roermund, C. W. T., Vervoorn, R. C., and Tager, J. M. (1986) *Biochem. J.* **237**, 379–389
16. Page, R. A., Kitson, K. E., and Hardman, M. J. (1991) *Biochem. J.* **278**, 659–665
17. Sola, M. M., Salto, R., Oliver, F. J., Gutiérrez, M., and Vargas, A. M. (1993) *J. Biol. Chem.* **268**, 19352–19357
18. Ren, J.-M., Marshall, B. A., Gulve, E. A., Gao, J., Johnson, D. W., Holloszy, J. O., and Mueckler, M. (1993) *J. Biol. Chem.* **268**, 16113–16115
19. Westerhoff, H. V., Groen, A. K., and Wanders, R. J. A. (1984) *Biosci. Rep.* **4**, 1–22
20. Brand, M. D., Hafner, R. P., and Brown, G. C. (1988) *Biochem. J.* **255**, 535–539
21. Hofmeyr, J. H., and Cornish-Bowden, A. (1991) *Eur. J. Biochem.* **200**, 223–236
22. Albe, K. R., and Wright, B. E. (1992) *J. Biol. Chem.* **267**, 3106–3114
23. Fell, D. A. (1992) *Biochem. J.* **286**, 313–330
24. Shiraishi, F., and Savageau, M. A. (1992) *J. Biol. Chem.* **267**, 22912–22918
25. Westerhoff, H. V., and Welch, G. R. (1992) *Curr. Top. Cell. Regul.* **33**, 361–390
26. Neely, J. R., Denton, R. M., England, P. J., and Randle, P. J. (1972) *Biochem. J.* **128**, 147–159
27. Simpson, I. A., and Cushman, S. W. (1986) *Annu. Rev. Biochem.* **55**, 1059–1089
28. Wheeler, T. J. (1988) *J. Biol. Chem.* **263**, 19447–19454
29. Slot, J. W., Geuze, H. J., Gigengack, S., James, D. E., and Lienhard, G. E. (1991) *Proc. Natl. Acad. Sci. U. S. A.* **88**, 7815–7819
30. Kolter, T., Uphues, L., Wichelhaus, A., Reinauer, H., and Eckel, J. (1992) *Biochem. Biophys. Res. Commun.* **189**, 1207–1214
31. Ren, J.-M., Semenkovich, C. F., Gulve, E. A., Gao, J., and Holloszy, J. O. (1994) *J. Biol. Chem.* **269**, 14396–14401
32. Krebs, H. A. (1961) *Biochem. J.* **80**, 225–233
33. Krebs, H. A. (1961) *Arch. Intern. Med.* **107**, 51–62
34. Taegtmeyer, H., Hems, R., and Krebs, H. A. (1980) *Biochem. J.* **186**, 701–711
35. Neely, J. R., Liebermeister, H., Battersby, E. J., and Morgan, H. E. (1967) *Am. J. Physiol.* **212**, 804–814
36. Masuda, T., Dobson, G. P., and Veech, R. L. (1990) *J. Biol. Chem.* **265**, 20321–20334
37. Langendorff, O. (1895) *Pflügers Arch. Gesamte Physiol. Menschen Tiere* **61**, 291–332
38. Ploug, T., Galbo, H., Vinten, J., Jorgensen, M., and Richter, E. A. (1987) *Am. J. Physiol.* **253**, E12–E20
39. Van Schaftingen, E., Lederer, B., Bartrons, R., and Hers, H.-G. (1982) *Eur. J. Biochem.* **129**, 191–195
40. Passonneau, J. V., and Lowry, O. H. (1993) in *Enzymatic Analysis: A Practical Guide*, Humana Press, Totowa, NJ
41. Goldberg, R. N., Tewari, Y. B., and Ahluwalia, J. C. (1989) *J. Biol. Chem.* **264**, 9901–9904
42. Tewari, Y. B., and Goldberg, R. N. (1991) *Biophys. Chem.* **40**, 59–67
43. Milner, Y., and Avigad, G. (1964) *Isr. J. Chem.* **2**, 316
44. Hestrin, S. (1949) *J. Biol. Chem.* **179**, 943–955
45. Lawson, J. W. R., Guynn, R. W., Cornell, N. W., and Veech, R. L. (1976) in *Gluconeogenesis: Its Regulation in Mammalian Species* (Hanson, R. W., and Mehlman, M. A., eds) pp. 481–514, John Wiley & Sons, New York
46. Guynn, R. W., Webster, L. T., Jr., and Veech, R. L. (1974) *J. Biol. Chem.* **249**, 3248–3254
47. Najjar, V. A. (1962) *Enzyme (Basel)* **6**, 161–178
48. Kahana, S. E., Lowry, O. H., Schulz, D. W., Passonneau, J. V., and Crawford, E. J. (1960) *J. Biol. Chem.* **235**, 2178–2184
49. Veech, R. L., Raijman, L., Dalziel, K., and Krebs, H. A. (1969) *Biochem. J.* **115**, 837–842
50. Hutter, O. F., and Noble, D. (1961) *J. Physiol. (Lond.)* **157**, 335–350
51. Cornell, N. W., Leadbetter, M., and Veech, R. L. (1979) *J. Biol. Chem.* **254**, 6522–6527
52. Lowry, O. H., and Passonneau, J. V. (1964) *J. Biol. Chem.* **239**, 31–42
53. McQuate, J. T., and Utter, M. F. (1959) *J. Biol. Chem.* **234**, 2151–2157
54. Williamson, D. H., Lund, P., Krebs, H. A. (1967) *Biochem. J.* **103**, 514–527
55. Passonneau, J. V., Schwartz, J. P., and Rottenberg, D. A. (1975) *J. Biol. Chem.* **250**, 2287–2292
56. Brown, D. H., and Cori, C. F. (1961) *Enzymes (Basel)* **5**, 207–228
57. Ganson, N. J., and Fromm, H. J. (1985) *J. Biol. Chem.* **260**, 12099–12105
58. Rose, Z. B., and Liebowitz, J. (1970) *Anal. Biochem.* **35**, 177–180
59. Clark, M. G. (1978) *Int. J. Biochem.* **9**, 17–18
60. Katz, J., and Rognstad, R. (1976) *Curr. Top. Cell. Regul.* **237**–289
61. Veloso, D., Guynn, R. W., Oskarsson, M. A., and Veech, R. L. (1973) *J. Biol. Chem.* **248**, 4811–4819
62. Veech, R. L., Gates, D. N., Crutchfield, C. W., Gitomer, W. L., Kashiwaya, Y., King, M. T., and Wondergem, R. (1994) *Alcohol. Clin. Exp. Res.*, in press
63. Veech, R. L., Nielsen, R., and Harris, R. L. (1975) in *Frontiers of Pineal Physiology* (Altschule, M. D., ed) pp. 177–196, MIT Press, Cambridge, MA
64. Michaelis, L., and Menten, M. L. (1913) *Biochem. Z.* **49**, 333–369
65. Kacser, H., and Burns, J. A. (1981) *Genetics* **97**, 639–666
66. Torres, N. V., Mateo, F., Meléndez-Hevia, E., and Kacser, H. (1986) *Biochem. J.* **234**, 169–174
67. Small, J. R. (1993) *Biochem. J.* **296**, 423–433
68. Thomas, S., and Fell, D. A. (1993) *Biochem. J.* **292**, 351–360
69. Walsh, D. A., Perkins, J. P., and Krebs, E. G. (1968) *J. Biol. Chem.* **243**, 3763–3765
70. Krebs, E. G., Graves, D. J., and Fischer, E. H. (1959) *J. Biol. Chem.* **234**, 2867–2873
71. Van Schaftingen, E., Hue, L., and Hers, H.-G. (1980) *Biochem. J.* **192**, 897–901
72. Uyeda, K., Furuya, E., and Luby, L. J. (1981) *J. Biol. Chem.* **256**, 8394–8399
73. Lawson, J. W. R., and Uyeda, K. (1987) *J. Biol. Chem.* **262**, 3165–3173
74. Depre, C., Rider, M. H., Veitch, K., and Hue, L. (1993) *J. Biol. Chem.* **268**, 13274–13279
75. Veech, R. L., Lawson, J. W. R., Cornell, N. W., and Krebs, H. A. (1979) *J. Biol. Chem.* **254**, 6538–6547
76. Lowry, O. H., Passonneau, J. V., Hasselberger, F. X., and Schulz, D. W. (1964) *J. Biol. Chem.* **239**, 18–30
77. Regen, D. M., and Pilkis, S. J. (1984) *J. Theor. Biol.* **111**, 635–658
78. Lueck, J. D., and Fromm, H. J. (1974) *J. Biol. Chem.* **249**, 1341–1347
79. Pilkis, S. J., El-Maghrabi, M. R., Pilkis, J., Claus, T. H., and Cumming, D. A. (1981) *J. Biol. Chem.* **256**, 3171–3174
80. Casazza, J. P., and Veech, R. L. (1986) *J. Biol. Chem.* **261**, 690–698
81. Kim, Y.-A., King, M. T., Teague, W. E., Rufo, G. A., Veech, R. L., and Passonneau, J. V. (1992) *Am. J. Physiol.* **262**, E344–E352
82. Estabrook, R. W., and Sacktor, B. (1958) *J. Biol. Chem.* **233**, 1014–1019